J|A|C|S
ARTICLES
Published on Web 12/12/2003

[Ni^0]-Catalyzed Co-oligomerization of 1,3-Butadiene and Ethylene: A Theoretical Mechanistic Investigation of Competing Routes for Generation of Linear and Cyclic C_{10}-Olefins

Sven Tobisch*

Contribution from the Institut für Anorganische Chemie der Martin-Luther-Universität Halle-Wittenberg, Fachbereich Chemie, Kurt-Mothes-Strasse 2, D-06120 Halle, Germany

Received October 4, 2003; E-mail: tobisch@chemie.uni-halle.de

Abstract: A detailed theoretical investigation of the mechanism for the [Ni^0]-catalyzed co-oligomerization of 1,3-butadiene and ethylene to afford linear and cyclic C_{10}-olefins is presented. Crucial elementary processes have been carefully explored for a tentative catalytic cycle, employing a gradient-corrected density functional theory (DFT) method. The favorable route for oxidative coupling starts from the prevalent [Ni^0-(η^2-butadiene)$_2$(ethylene)] form of the active catalyst through oxidative coupling between the two η^2-butadienes. The initial η^3,η^1(C^1)-octadienediyl−Ni^{II} product is the active precursor for ethylene insertion, which preferably takes place into the *syn*-η^3-allyl−Ni^{II} bond of the prevalent η^3-*syn*,η^1(C^1),Δ-*cis* isomer. The insertion is driven by a strong thermodynamic force, giving rise entirely to η^3,η^1,Δ-*trans*-decatrienyl−Ni^{II} forms, with the η^3-*anti*,η^1,Δ-*trans* isomer almost exclusively generated. Occurrence of allyl,η^1,Δ-*cis* isomers, however, is precluded on both kinetic and thermodynamic grounds, thereby rationalizing the observation that *cis*-DT and *cis*,*cis*-CDD are never formed. Linear and cyclic C_{10}-olefins are generated in a highly stereoselective fashion, with *trans*-DT and *cis*,*trans*-CDD as the only isomers, along competing routes of stepwise transition-metal-assisted H-transfer (DT) and reductive CC elimination under ring closure (CDD), respectively, that start from the prevalent η^3-*anti*,η^1,Δ-*trans*-decatrienyl−Ni^{II} species. The role of allylic conversion in the octadienediyl−Ni^{II} and decatrienyl−Ni^{II} complexes has been analyzed. As a result of the detailed exploration of all important elementary steps, a theoretically verified, refined catalytic cycle is proposed and the regulation of the selectivity for formation of linear and cyclic C_{10}-olefins is elucidated.

Introduction

Zerovalent nickel complexes have been demonstrated by the comprehensive and systematic investigations of Wilke and co-workers[1,2] as versatile and useful catalysts for the cyclooligomerization of 1,3-butadiene. Depending on the actual structure of the active catalyst species, nickel complexes support the generation of C_8-cycloolefins [with 4-vinylcyclohexene (VCH) and *cis*,*cis*-cycloocta-1,5-diene (*cis*,*cis*-COD) as major products] and of C_{12}-cycloolefins [with *trans*,*trans*,*trans*-cyclododeca-1,5,9-triene (*all-t*-CDT) as the predominant product] along different reaction channels that involve the linkage of two or three butadiene moieties, respectively.[3] Much of the mechanistic understanding of this intriguing reaction is largely due to the fundamental work of Wilke and co-workers.[1−3] Their first proposed mechanism has been recently confirmed in essential details but supplemented, in a series of theoretical mechanistic investigations,[4] by novel insights into how the catalytic 1,3-butadiene cyclooligomerization reaction operates.

The nickel complexes used for 1,3-butadiene cyclooligomerization are known also to catalyze the formation of co-oligomers between 1,3-dienes and olefins. For the zerovalent "bare" nickel complex (for instance, [Ni^0(COD)$_2$]), the 1,3-butadiene cyclooligomerization affording C_{12}-cycloolefins is largely impeded in the presence of ethylene and instead C_{10}-olefins (viz. 2:1 butadiene/ethylene co-oligomers) are formed.[5] The product mixture contains both cyclic, namely cyclodeca-1,5-diene

(1) (a) Jolly, P. W.; Wilke, G. The Oligomerization and Co-oligomerization of Butadiene and Substituted 1,3-Dienes. In *The Organic Chemistry of Nickel, Vol. 2, Organic Synthesis*; Academic Press: New York, 1975; pp 133−212. (b) Jolly, P. W. Nickel-Catalyzed Oligomerization of 1,3-Dienes Related Reactions. In *Comprehensive Organometallic Chemistry*; Wilkinson, G., Stone, F. G. A., Abel, E. W., Eds.; Pergamon: New York, 1982; Vol. 8, pp 671−711. (c) Keim, W.; Behr, A.; Röper, M. Alkene and Alkyne Oligomerization, Cooligomerization and Telomerization Reactions. In *Comprehensive Organometallic Chemistry*; Wilkinson, G., Stone, F. G. A., Abel, E. W., Eds.; Pergamon: New York, 1982; Vol. 8, pp 371−462. (d) Heimbach, P.; Jolly, P. W.; Wilke, G. *Adv. Organomet. Chem.* **1970**, *8*, 29. (e) Baker, R. *Chem. Rev.* **1973**, *73*, 487.

(2) (a) Wilke, G. *Angew. Chem., Int. Ed. Engl.* **1963**, *2*, 105. (b) Wilke, G. *Angew. Chem., Int. Ed. Engl.* **1988**, *27*, 185. (c) Wilke, G.; Eckerle, A. Cyclooligomerizations and Cyclo-Co-Oligomerizations of 1,3-Dienes. In *Applied Homogeneous Catalysis with Organometallic Complexes*; Cornils, B., Herrmann, W. A., Eds.; VCH: Weinheim, Germany, 2002; pp 368−382.

(3) (a) Bogdanovic, B.; Heimbach, P.; Kröner, M.; Wilke, G. *Justus Liebigs Ann. Chem.* **1969**, *727*, 143. (b) Brenner, W.; Heimbach, P.; Hey, H.; Müller, E. W.; Wilke, G. *Justus Liebigs Ann. Chem.* **1969**, *727*, 161. (c) Heimbach, P.; Kluth, J.; Schlenkluhn, H.; Weimann, B. *Angew. Chem., Int. Ed. Engl.* **1980**, *19*, 569. (d) Heimbach, P.; Kluth, J.; Schlenkluhn, H.; Weimann, B. *Angew. Chem., Int. Ed. Engl.* **1980**, *19*, 570. (e) Benn, R.; Büssemeier, B.; Holle, S.; Jolly, P. W.; Mynott, R.; Tkatchenko, I.; Wilke, G. *J. Organomet. Chem.* **1985**, *279*, 63.

(4) (a) Tobisch, S.; Ziegler, T. *J. Am. Chem. Soc.* **2002**, *124*, 4881. (b) Tobisch, S.; Ziegler, T. *J. Am. Chem. Soc.* **2002**, *124*, 13290. (c) Tobisch, S. *Chem. Eur. J.* **2003**, *9*, 1217. (d) Tobisch, S. *Adv. Organomet. Chem.* **2003**, *49*, 167.

Scheme 1. Tentative Catalytic Cycle of the [Ni^0]-Catalyzed Co-oligomerization of 1,3-Butadiene and Ethylene Affording Linear and Cyclic C_{10}-Olefin Products[a]

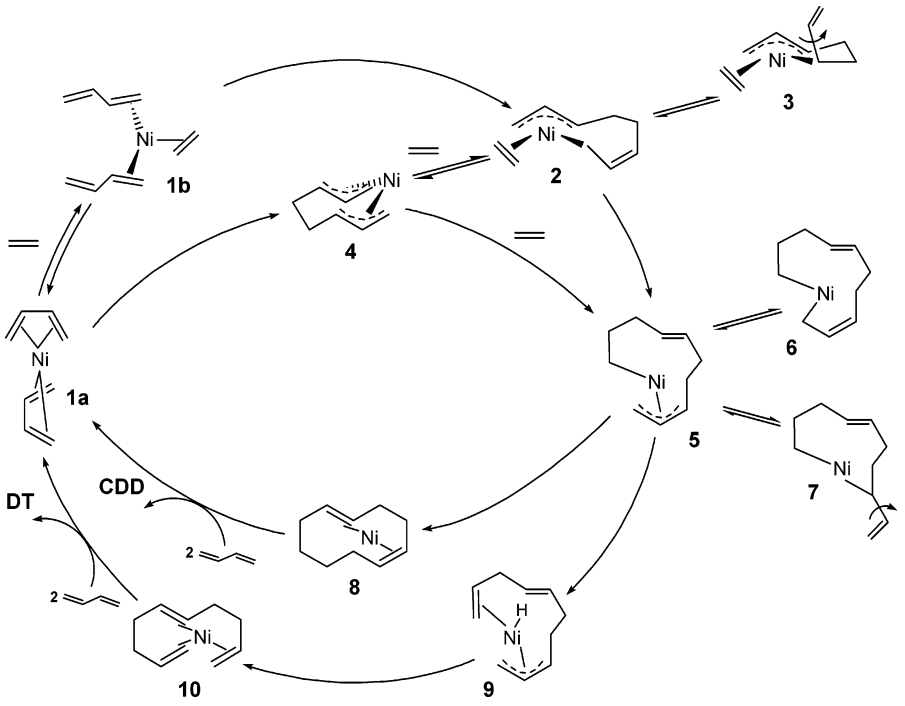

[a] Based on experimental studies of Wilke et al.[5] Please note that only the favorable forms of **1a** and **1b** are shown.

(CDD), and linear, namely deca-1,4,9-triene (DT), C_{10}-olefins as the principal products. The co-oligomerization occurs in a highly stereoselective fashion, such that cyclodeca-*cis*-1,*trans*-5-diene (*cis*,*trans*-CDD) and deca-1,*trans*-4,9-triene (*trans*-DT) are the exclusively generated C_{10}-olefins among the several possible isomers. The reaction temperature as well as the butadiene-to-ethylene ratio has been found to decisively influence the product distribution. For a 1:1 reactant ratio, low temperatures favors the generation of *cis*,*trans*-CDD (CDD:DT ~7:3 at 40 °C), while at elevated temperatures *trans*-DT is prevalent (CDD:DT ~3:7 at 80 °C). The C_{10}-olefin proportion enlarges with the relative increase of the ethylene concentration, which serves to almost entirely suppress the generation of C_{12}-cycloolefins as side products.

Similar to the nickel-catalyzed 1,3-butadiene cyclooligomerization, the co-oligomerization of 1,3-butadiene and ethylene occurs in a multistep fashion. The nickel atom template undergoes a repeated change in its formal oxidation state, namely [$Ni^0 \rightleftharpoons Ni^{II}$], during the multistep addition−elimination mechanism. The reaction course of the co-oligomerization, however, is not completely understood so far. Scheme 1 displays a tentative catalytic cycle of the [Ni^0]-catalyzed process, which is based on the experimental studies of Wilke et al.[5] The zerovalent olefin−Ni^0 catalyst complex can exist in several forms of either the [Ni^0(olefin)$_2$] compound **1a** or the [Ni^0(olefin)$_3$] compound **1b**, where the catalytically active species possesses two coordinated butadienes. The first step involves the oxidative coupling of two butadiene moieties giving rise to the octadienediyl−Ni^{II} complex, which may be coordinatively saturated by complexation of further olefins. This complex occurs in various configurations, which are distinguished by the coordination mode of the octadienediyl framework, viz. the $\eta^3,\eta^1(C^1)$ species **2**, the $\eta^3,\eta^1(C^3)$ species **3**, and the bis(η^3) species **4**, all of which can be assumed to be in equilibrium. Ethylene insertion into the allyl−Ni^{II} bond in either of the octadienediyl−Ni^{II} species, with **4** suggested to be the active precursor,[5] leads to the decatrienyl−Ni^{II} complex. Similar to the octadienediyl−Ni^{II} complex, the decatrienyl−Ni^{II} complex is present as species **5**, **6**, and **7**, with the allylic group in the η^3-π, $\eta^1(C^1)$-σ, and $\eta^1(C^3)$-σ modes. Either one of these species can be considered as the precursor for production of both CDD and DT, respectively. The [Ni^0(CDD)] product **8** is formed by reductive elimination under ring closure via formation of a C−C σ-bond between the η^1-alkyl group and the terminal allylic carbon, with **5** suggested to be the precursor.[5] The generation of DT, however, requires a hydrogen atom to be transferred. This is likely to proceed by β-H abstraction from the alkyl group, which was envisaged to involve the σ-allyl species **7**, giving rise to a hydrido−Ni^{II} intermediate **9**, and subsequent reductive CH elimination to afford the [Ni^0(DT)] product **10**. The several isomers of CDD and DT are formed through competing pathways along **5** → **8** and **5** → **10**, respectively, that involve different stereoisomers. Displacement of the C_{10}-olefin products in subsequent consecutive kinetically facile substitution steps with butadiene regenerates the active catalyst, thereby completing the catalytic cycle.

The plausibility of this tentative reaction cycle is supported by stoichiometric reactions and is underlined because of its great similarity to the well-established catalytic course of butadiene

(5) (a) Heimbach, P.; Wilke, G. *Justus Liebigs Ann. Chem.* **1969**, *727*, 183. (b) The following reaction conditions were found to be optimal for the catalytic co-oligomerization of 1,3-butadiene and ethylene: 1,3-butadiene and ethylene in a 1:1 molar ratio at 20 °C and 20−30 atm pressure, bare Ni^0 complexes (for instance, [Ni^0(COD)$_2$]) as catalyst, benzene as solvent. At these conditions the product mixture predominantly consists of *cis*,*trans*-CDD (~88%) with *trans*-DT is formed in a lower portion (~12%). (c) For 1,3-butadiene and ethylene in a 1:1 molar ratio the co-oligomerization to yield C_{10}-olefins has been observed to occur at an overall reaction rate that is approximately 6 times larger when compared to the competing cyclooligomerization affording C_{12}-cycloolefins.

cyclooligomerization.[1−4] Formal 16e$^-$ or 18e$^-$ forms of **1a** and **1b**, respectively, can be envisaged as likely candidates for the active catalyst, although it has been never experimentally characterized. A [Ni^0(η^4-*cis*-2,3-dimethylbutadiene)$_2$] complex,[6] with two tetrahedrally coordinated *cis*-butadienes, and also the [Ni^0(ethylene)$_3$] complex[7] are well-known. The various octadienediyl−Ni^{II} configurations, as well as their facile mutual rearrangement,[3e] have been firmly established for the PR$_3$/P(OR)$_3$-stabilized complex.[3e,6a,8] Bis(η^1)-octadienediyl−Ni^{II} species, although conceivable as reactive intermediates for allylic conversion and ethylene insertion processes, are not likely to be involved in any of these steps. They have been demonstrated to be energetically highly unfavorable and seen to play no role in the cyclooligomerization reaction.[4] Indirect evidence for the intermediacy of the octadienediyl−Ni^{II} complex comes from the stereochemistry of the products generated by the co-oligomerization of piperylene (1,3-pentadiene) with ethylene and by piperylene cyclodimerization. The configuration of the methyl groups in the cyclooligomer's 10-membered ring was found to be identical to that observed in the methyl-substituted divinylcyclobutane cyclodimerization product.[1a,9] Accordingly, the octadienediyl−Ni^{II} complex, which is a well-established intermediate of the 1,3-butadiene cyclooligomerization,[1−4] is likely to be also involved in the co-oligomerization reaction course. Although not directly observed for alkenes, insertion of analogous alkynes into the allyl−Ni bond of the octadienediyl−Ni^{II} complex has been observed in stoichiometric reactions, leading to the isolation of the related insertion product as well as of the corresponding cyclic co-oligomer.[10] Further evidence comes from the experimental observation that the formation of linear co-oligomers is entirely suppressed for the process involving substituted alkenes or alkynes, in which β-hydrogen atoms are absent.[1a]

On the basis of the tentative catalytic cycle, the present theoretical mechanistic investigation is aimed at extending the understanding of the Ni^0-catalyzed co-oligomerization of 1,3-butadiene and ethylene, affording C$_{10}$-olefins, by elucidating the following intriguing but not yet firmly resolved aspects:

(1) What is the thermodynamically favorable and the catalytically active form of the catalyst complex?

(2) In what fashion does the oxidative coupling preferably take place and which of the various octadienediyl−Ni^{II} forms is generated initially?

(3) Which of the various configurations of the octadienediyl−Ni^{II} and the decatrienyl−Ni^{II} complexes are the thermodynamically preferred ones, respectively, and which of them act as the precursor for the ethylene insertion and for C$_{10}$-co-oligomer formation along the CDD- and DT-generating routes?

(4) Which of the isomeric syn or anti forms of the allyl−Ni^{II} bond of the octadienediyl−Ni^{II} intermediate display a higher proclivity to undergo ethylene insertion, and does the insertion preferably occur into the η^3- or the η^1-allyl−Ni^{II} bond?

(5) Does the competitive production of CDD and DT commence from identical or different configurations of the decatrienyl−Ni^{II} complex as the precursor?

(6) Does the hydrogen transfer along the DT route take place in a stepwise or a concerted fashion; i.e., is a hydrido−Ni^{II} intermediate involved along the most feasible pathway?

(7) Which factors control the selective formation of only one of the several possible stereoisomers of the principal CDD and DT products, viz. *cis*,*trans*-CDD and *trans*-DT, respectively?

(8) What are the critical factors that regulate the selectivity for formation of linear and cyclic C$_{10}$-olefins?

The present computational study is, to the best of our knowledge, the first detailed comprehensive theoretical mechanistic investigation of the complete reaction cycle for the catalytic co-oligomerization of 1,3-butadiene and ethylene to yield C$_{10}$-olefins, mediated by zerovalent bare nickel complexes. This represents a further part of our systematic theoretical exploration of crucial structure−reactivity relationships in transition-metal-assisted oligomerization reactions of 1,3-dienes.[4]

Computational Model and Method

Model. The entire catalytic cycle of the [Ni^0]-catalyzed co-oligomerization of 1,3-butadiene and ethylene consisting of the critical elementary steps displayed in Scheme 1 was investigated. These critical elementary steps are oxidative coupling of two butadienes; allylic isomerization and enantioface conversion occurring in the octadienediyl−Ni^{II} and decatrienyl−Ni^{II} complexes, respectively; ethylene insertion into the allyl−Ni^{II} bond of the octadienediyl−Ni^{II} complex; and reductive CC elimination under ring closure as well as transition-metal-assisted H-transfer commencing from the decatrienyl−Ni^{II} complex. Various conceivable paths for individual elementary steps have been explored. Furthermore, the several possible stereochemical pathways, which originate from the enantioface and the configuration (s-trans or s-cis) of the prochiral butadiene moieties involved, have been carefully examined for the favorable route for each of the critical elementary steps (cf. Labeling of the Molecules section).

Method. All reported DFT calculations were performed by using the TURBOMOLE program package developed by Häser and Ahlrichs and co-workers.[11] The local exchange-correlation potential by Slater[12a,b] and Vosko et al.[12c] was augmented with gradient-corrected functionals for electron exchange according to Becke[12d] and correlation according to Perdew[12e] in a self-consistent fashion. This gradient-corrected density functional is usually termed BP86 in the literature. In recent benchmark computational studies it was shown that the BP86 functional gives results in excellent agreement with the best wave function-based methods available today, for the class of reactions investigated here.[13] The applied computational methodology has furthermore been demonstrated to reproduce the total activation barrier ($\Delta G^{\ddagger}_{tot}$) for nickel-catalyzed 1,3-butadiene cyclooligomerization reactions with an accuracy of ∼1−2 kcal mol^{-1} when compared with experiment.[4b,c]

For all atoms a standard all-electron basis set of triple-ζ quality for the valence electrons augmented with polarization functions was employed for the geometry optimization and the saddle-point search.

(6) (a) Jolly, P. W.; Mynott, R.; Salz, R. *J. Organomet. Chem.* **1980**, *184*, C49. (b) Jolly, P. W.; Mynott, R. *Adv. Organomet. Chem.* **1981**, *19*, 257.
(7) Fischer, K.; Jonas, K.; Wilke, G. *Angew. Chem., Int. Ed. Engl.* **1973**, *12*, 565.
(8) (a) Jolly, P. W.; Tkatchenko, I.; Wilke, G. *Angew. Chem., Int. Ed. Engl.* **1971**, *10*, 329. (b) Brown, J. M.; Golding, B. T.; Smith, M. J. *J. Chem. Soc., Chem. Commun.* **1971**, 1240. (c) Barnett, B.; Büssemeier, B.; Heimbach, P.; Jolly, P. W.; Krüger, C.; Tkatchenko, I.; Wilke, G. *Tetrahedron Lett.* **1972**, 1457.
(9) Heimbach, P. *Angew. Chem., Int. Ed. Engl.* **1973**, *12*, 975.
(10) Büssemeier, B.; Jolly, P. W.; Wilke, G. *J. Am. Chem. Soc.* **1974**, *64*, 4726.
(11) (a) Ahlrichs, R.; Bär, M.; Häser, M.; Horn, H.; Kölmel, C. *Chem. Phys. Lett.* **1989**, *162*, 165. (b) Treutler, O.; Ahlrichs, R. *J. Chem. Phys.* **1995**, *102*, 346. (c) Eichkorn, K.; Treutler, O.; Öhm, H.; Häser, M.; Ahlrichs, R. *Chem. Phys. Lett.* **1995**, *242*, 652.
(12) (a) Dirac, P. A. M. *Proc. Cambridge Philos. Soc.* **1930**, *26*, 376. (b) Slater, J. C. *Phys. Rev.* **1951**, *81*, 385. (c) Vosko, S. H.; Wilk, L.; Nussiar, M. *Can. J. Phys.* **1980**, *58*, 1200. (d) Becke, A. D. *Phys. Rev.* **1988**, *A38*, 3098. (e) Perdew, J. P. *Phys. Rev.* **1986**, *B33*, 8822; *Phys. Rev. B* **1986**, *34*, 7406.
(13) (a) Bernardi, F.; Bottoni, A.; Calcinari, M.; Rossi, I.; Robb, M. A. *J. Phys. Chem.* **1997**, *101*, 6310. (b) Jensen, V. R.; Børve, K. *J. Comput. Chem.* **1998**, *19*, 947.

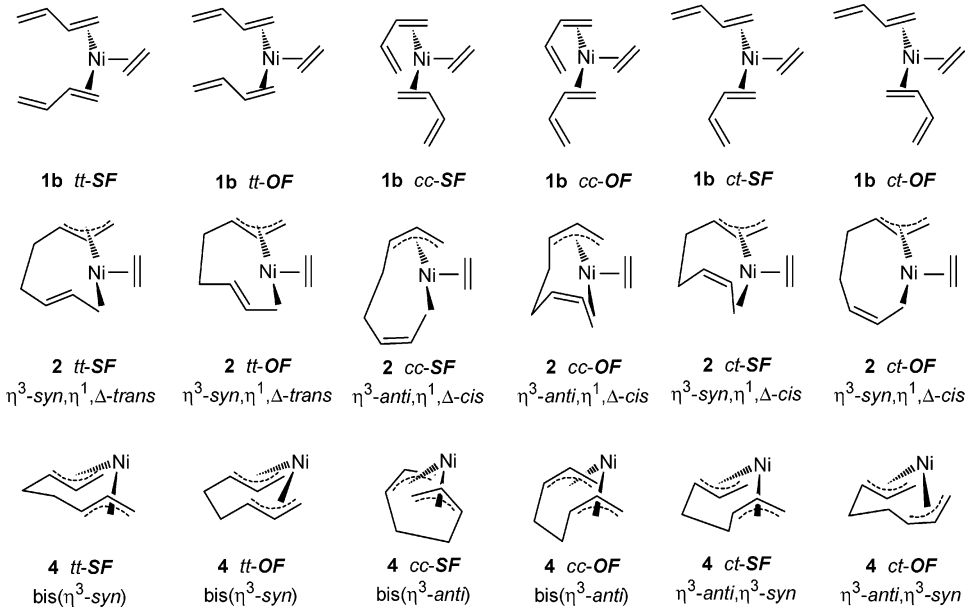

Figure 1. Stereoisomeric forms of the [Ni^0(η^2-butadiene)$_2$(ethylene)] catalyst complex **1b**, together with the related stereoisomers of the η^3,η^1(C^1)- and bis(η^3)-octadienediyl−Ni^{II} species **2** and **4**, respectively. For notation see the text.

The Wachters 14s/9p/5d set[14a] supplemented by two diffuse p[14a] and one diffuse d function[14b] contracted to (62111111/5111111/3111) was used for nickel, and standard TZVP basis sets[14c] were used for carbon [a 10s/6p/1d set contracted to (7111/411/1)] and for hydrogen [a 5s/1p set contracted to (311/1)]. The frequency calculations were done by using standard DZVP basis sets,[14c] which consist of a 15s/9p/5d set contracted to (63321/531/41) for nickel, a 9s/5p/1d set contracted to (621/41/1) for carbon, and a 5s set contracted to (41) for hydrogen, for DZVP-optimized structures, which differ to a marginal extent from the triple-ζ-optimized ones. The corresponding auxiliary basis sets were used for fitting the charge density.[14c,d]

Stationary Points. The geometry optimization and the saddle-point search were carried out at the BP86 level of approximation by utilizing analytical/numerical gradients/Hessians according to standard algorithms. No symmetry constraints were imposed in any case. The stationary points were identified exactly by the curvature of the potential-energy surface at these points corresponding to the eigenvalues of the Hessian. All reported transition states possess exactly one negative Hessian eigenvalue, while all other stationary points exhibit exclusively positive eigenvalues. The educt and product that correspond directly to the located transition-state structure were verified by following the reaction pathway going downhill to both sides from slightly relaxed transition-state structures. The reaction and activation enthalpies and free energies (ΔH, $\Delta H^{\ddagger}$, ΔG, and $\Delta G^{\ddagger}$ at 298 K and 1 atm) were evaluated according to standard textbook procedures[15] using computed harmonic frequencies.

The co-oligomerization reaction occurs in liquid phase.[5b] Accordingly, the $T\Delta S$ contribution of ∼11−13 kcal mol^{-1} (298.15 K, 1 atm) calculated for ethylene or butadiene coordination in gas phase certainly does not reflect the real entropic cost for association and dissociation processes involving additional ethylene or butadiene monomers under actual catalytic reaction conditions.[5b] The gas-phase entropies have to at least be corrected by the vaporization entropy (for instance, ΔS^{LV} = 20.1 eu for butadiene).[16] This reduces the entropic costs, for example, for butadiene association, by 6.0 kcal mol^{-1} (298.15 K); thus to approximately half of the gas-phase value. This estimation agrees quite well with the findings of a recent theoretical study, where it was shown that the entropies in solution are decreasing to nearly half of the gas-phase value.[17] Therefore, the solvation entropy for monomer coordination was approximated as being half of its gas-phase value, which is considered as a reliable estimate of the entropy contribution in condensed phase.

Labeling of the Molecules. Important species of the catalytic cycle were labeled with the arabic numbers given in Scheme 1. The several stereoisomeric pathways possible for each of the individual steps were classified according to the kind of butadiene coupling to which the stereoisomeric form of the precursor corresponded. The following notation was applied. The butadiene coupling can occur between identical configurations, viz., two *cis*-butadienes (*c*/*c*) or two *trans*-butadienes (*t*/*t*), or between two butadienes of different configuration (*t*/*c*) with either the same (denoted SF; i.e., same face) or the opposite (denoted OF; i.e., opposite face) enantioface of the two butadienes involved. The respective stereoisomers of the active catalyst complex are schematically depicted in Figure 1 for **1b** as an example, together with the related octadienediyl−Ni^{II} species **2** and **4**, respectively.

Results and Discussion

The theoretical mechanistic investigation of the catalytic co-oligomerization reaction starts with the careful step-by-step exploration of the elementary processes outlined in Scheme 1. This examination is aimed at enlightening the crucial features of each of the individual steps and to propose the most feasible of the various conceivable paths. From the detailed insight achieved for the critical elementary steps, a condensed mechanistic scheme comprised of thermodynamic and kinetic aspects for the respective favorable pathways is presented and the mechanistic implications for the selectivity control are elucidated.

I. Exploration of Crucial Elementary Steps. A. Oxidative Coupling of Two Butadienes Affording the Octadienediyl−Ni^{II} Complex. First, the several possible forms of the active catalyst complex are investigated in order to infer the thermo-

(14) (a) Wachters, A. H. J. *J. Chem. Phys.* **1970**, *52*, 1033. (b) Hay, P. J. *J. Chem. Phys.* **1977**, *66*, 4377. (c) Godbout, N.; Salahub, D. R.; Andzelm, J.; Wimmer, E. *Can. J. Chem.* **1992**, *70*, 560. (d) TURBOMOLE basis set library.

(15) McQuarrie, D. A. *Statistical Thermodynamics*; Harper & Row: New York, 1973.

(16) Lide, D. R.; Ed. *CRC Handbook of Chemistry and Physics*, 76th ed.; CRC Press: Boca Raton, FL, 1995.

(17) Cooper, J.; Ziegler, T. *Inorg. Chem.* **2002**, *41*, 6614.

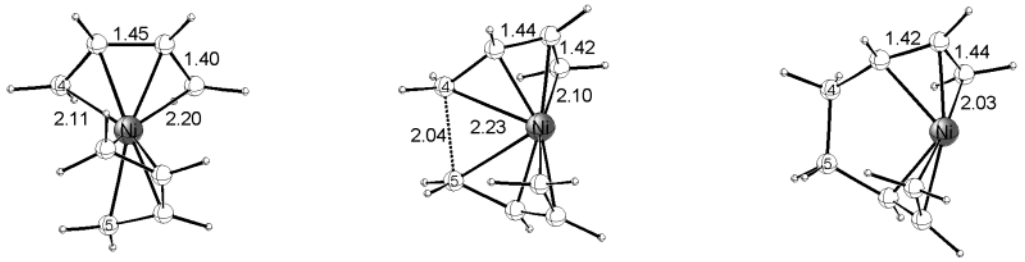

bis(η^4-*cis*)-BD **1a** TS[**1a**-**4**] bis(η^3-*anti*) **4**

Figure 2. Selected geometric parameters (angstroms) of the optimized structures of key species for oxidative coupling via the most feasible pathway for η^4-*cis*/η^4-*cis*-butadiene coupling along **1a** → **4**.

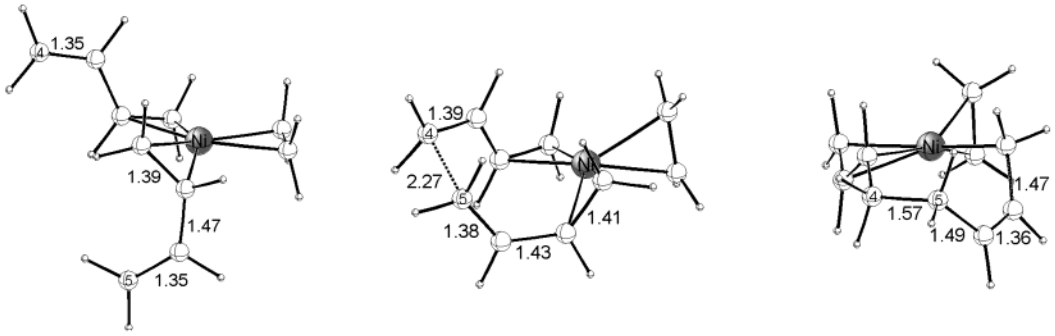

η^2-*trans*/η^2-*cis*-BD **1b** TS[**1b**-**2**] η^3-*syn*,η^1(C^1),Δ-*cis* **2**

Figure 3. Selected geometric parameters (angstroms) of the optimized structures of key species for oxidative coupling via the most feasible pathway for η^2-*trans*/η^2-*cis*-butadiene (OF) coupling along **1b** → **2**.

Table 1. Thermodynamic Stability of the Most Favorable Isomers of the [Ni^0(olefin)$_2$] **1a** and [Ni^0(olefin)$_3$] **1b** Complexes[a]

isomer	Δ*H*/ΔG,[a] kcal mol^{-1}
η^4-*t*,η^2-*t*-BD **1a**	8.7/*2.8*
bis(η^4-*c*-BD) **1a**	8.0/*2.9*
bis(η^2-*t*-BD),ethene **1b**	0.0/*0.0*
tris(η^2-*t*-BD) **1b**	1.8/*2.0*
tris(ethene) **1b**	−4.4/*−4.6*
bis(ethene),η^2-*t*-BD **1b**	−1.7/*−1.8*
bis(ethene),η^4-*c*-BD **1b**	0.7/*1.1*
bis(η^2-*t*-BD),η^4-*c*-BD **1b**	5.1/*5.8*
η^2-*t*-BD,ethene,η^4-*c*-BD **1b**	2.5/*3.7*

[a] Gibbs free energies are shown in italic type.

dynamically favorable one, which is followed by the investigation of their proclivity to undergo oxidative coupling. Based on the precedence of known olefin−Ni^0 complexes,[6,7] the two butadienes can be coordinated in bis(η^4) and η^4,η^2 mode for **1a**, while tris(ethylene)−Ni^0, tris(η^2-butadiene)−Ni^0, bis(η^2-butadiene)(ethylene)−Ni^0, bis(ethylene)(η^2-butadiene)−Ni^0, bis-(η^2-butadiene)(η^4-butadiene)−Ni^0, bis(ethylene)(η^4-butadiene)−Ni^0, and (η^2-butadiene)(ethylene)(η^4-butadiene)−Ni^0 compounds are possible $16e^-$ and $18e^-$ species, respectively, of **1b**. The relative thermodynamic stability of the most favorable isomers for each of these forms is reported in Table 1. Among the several forms of **1a** and **1b**, all of which are assumed to be in equilibrium, the tris(ethylene)−Ni^0 species is seen to be favorable. This, however, is a dormant species. The higher stability of ethylene complexation relative to coordination of butadiene, which, for example, amounts to 6.6 kcal mol^{-1} (Δ*G*) for tris(ethylene)−Ni^0 vs tris(η^2-*trans*-butadiene)−Ni^0 species, is essentially attributed to unfavorable steric interactions, which act to prevent the preferred trigonal planar conformation for the latter species. Concerning the catalytically active forms with two (or more) coordinated butadienes, the formal $16e^-$ trigonal planar [Ni^0(η^2-butadiene)$_2$(ethylene)] compound, with butadiene preferably coordinated in the η^2-*trans* mode, is predicted to be prevalent. The related [Ni^0(η^2-butadiene)$_3$] compound is energetically unfavored by 2.0 kcal mol^{-1} (Δ*G*). The other active forms of **1a** and **1b**, respectively, should also occur in appreciable but smaller concentrations, as they are ∼2.8−5.8 kcal mol^{-1} higher in free energy.

Various paths for oxidative coupling that commence from the different active forms of **1a** and **1b**, respectively, were probed. Two feasible coupling routes have been found. The bis-(η^4)-butadiene form of **1a** is the precursor for the first **1a** → **4** route, giving rise to the bis(η^3)-octadienediyl−Ni^{II} species **4** as the directly generated coupling product (cf. Figure 2). The formation of a new C−C σ-bond between two bidentate-coordinated butadienes occurs via the productlike transition state TS[**1a**−**4**], where the two allylic moieties are almost completely preformed. The same kind of transition state is encountered when starting from the η^4,η^2-butadiene form of **1a**. Therefore, the coupling occurring between two η^4-butadienes along **1a** → **4** is favorable for all forms of **1a**. The second coupling route is assisted by ethylene. Commencing from the [Ni^0(η^2-butadiene)$_2$-(ethylene)] form of **1b**, the oxidative coupling proceeds via establishment of a new C−C bond between the terminal noncoordinated carbons C^4 and C^5 of two η^2-butadienes (cf. Figure 3), that occurs at a distance of ∼2.2−2.3 Å in the eductlike transition state TS[**1b**−**2**]. The η^3,η^1(C^1)-octadiene-diyl−Ni^{II} species **2** is formed as the initial coupling product. This route is energetically preferred for all active forms of **1b**,

Table 2. Activation Enthalpies and Free Energies and Reaction Enthalpies and Free Energies for Oxidative Coupling of Two η^4-Butadienes along **1a** → **4**, with the [$Ni^0(\eta^4$-butadiene$)_2$] Species **1a** as Precursor[a–d]

	BD coupling path		
BD coupling isomer[e]	**1a**	TS[**1a**–**4**]	**4**
cis,*cis*-BD	bis(η^4-*cis*-BD)		bis(η^3-*anti*)
c/*c*-BD SF	8.0/*2.9*	**26.8**/***22.6***	11.9/*7.7*
c/*c*-BD OF	8.0/*2.9*	33.9/*29.6*	5.0/*0.6*
trans,*cis*-BD	η^4-*trans*,η^4-*cis*-BD		η^3-*syn*,η^3-*anti*
t/*c*-BD SF	14.5/*8.8*	54.2/*49.6*	7.3/*3.0*
t/*c*-BD OF	14.5/*8.8*	40.6/*36.1*	
trans,*trans*-BD	bis(η^4-*trans*-BD)		bis(η^3-*syn*)
t/*t*-BD SF	15.4/*9.8*	63.2/*58.6*	2.8/−*1.5*
t/*t*-BD OF	15.4/*9.8*		6.1/*1.5*

[a] This process is classified according to the kind of butadiene coupling involved. The relationship between the butadiene coupling and the stereoisomers of **4** is explicitly given. [b] Total barriers and reaction energies are relative to the most stable isomer of the [$Ni^0(\eta^2$-butadiene$)_2$(ethylene)] active catalyst species **1b**, namely, [$Ni^0(\eta^2$-*trans*-butadiene$)_2$(ethylene)]. [c] Activation enthalpies and free energies ($\Delta H^{\ddagger}/\Delta G^{\ddagger}$) and reaction enthalpies and free energies ($\Delta H/\Delta G$) are given in kilocalories per mole; numbers in italic type are the Gibbs free energies. [d] The lowest barrier for the individual stereochemical pathway is shown in boldface type. [e] See the text section Labeling of the Molecules.

Table 3. Activation Enthalpies and Free Energies and Reaction Enthalpies and Free Energies for Oxidative Coupling of Two η^2-Butadienes along **1b** → **2**, with the [$Ni^0(\eta^2$-butadiene$)_2$-(ethylene)] Species **1b** as Precursor[a–d]

	BD coupling path		
BD coupling isomer[e]	**1b**	TS[**1b**–**2**]	**2**
cis,*cis*-BD	bis(η^2-*cis*-BD)		η^3-*anti*,$\eta^1(C^1)$,Δ-*cis*
c/*c*-BD SF	5.0/*4.4*	15.8/*17.7*	−1.7/*0.9*
c/*c*-BD OF	6.4/*5.9*	25.5/*27.0*	3.3/*5.9*
trans,*cis*-BD	η^2-*trans*,η^2-*cis*-BD		η^3-*syn*,$\eta^1(C^1)$,Δ-*cis*
t/*c*-BD SF	3.0/*2.6*	18.1/*19.6*	0.0/*2.6*
t/*c*-BD OF	3.3/*3.0*	**10.7**/***12.8***	**−2.7**/−***0.1***
trans,*trans*-BD	bis(η^2-*trans*-BD)		η^3-*syn*,$\eta^1(C^1)$,Δ-*trans*
t/*t*-BD SF	0.0/*0.0*	13.4/*15.5*	9.7/*12.4*
t/*t*-BD OF	1.0/*0.5*	16.6/*18.3*	14.9/*17.5*

[a] This process is classified according to the kind of butadiene coupling involved. The relationship between the butadiene coupling and the stereoisomers of **2** is explicitly given. [b] Total barriers and reaction energies are relative to the most stable isomer of the [$Ni^0(\eta^2$-butadiene$)_2$(ethylene)] active catalyst species **1b**, namely, [$Ni^0(\eta^2$-*trans*-butadiene$)_2$(ethylene)]. [c] Activation enthalpies and free energies ($\Delta H^{\ddagger}/\Delta G^{\ddagger}$) and reaction enthalpies and free energies ($\Delta H/\Delta G$) are given in kilocalories per mole; numbers in italic type are the Gibbs free energies. [d] The lowest barrier for the individual stereochemical pathway is shown in boldface type. [e] See the text section Labeling of the Molecules.

since the η^4,η^2-butadiene isomers of **1b** are found to approach the corresponding bis(η^2)-butadiene isomers in the vicinity of the transition state.

The energetics of the oxidative coupling is primarily determined by the configuration and the enantioface of the two reacting butadiene moieties (Tables 2 and 3). Identical stereochemical pathways are found to be kinetically preferred along **1a** → **4** and **1b** → **2** for coupling of *c*/*c*-butadiene (SF coupling), *t*/*t*-butadiene (SF coupling), and *t*/*c*-butadiene (OF coupling). For the **1a** → **4** route, the thermodynamically most stable bis(η^4-*cis*) isomer is also seen to be kinetically preferred by the overall lowest total barrier of 22.6 kcal mol^{-1} ($\Delta G^{\ddagger}$ relative to **1b**, Table 2), while the *t*/*c*- and *t*/*t*-butadiene coupling require significantly higher barriers. Thus, these stereochemical pathways are almost entirely precluded and the bis(η^3-*anti*) isomer of **4** would be exclusively formed along this route. The coupling of *t*/*c*-η^2-butadiene (OF coupling) is favorable along **1b** → **2** among the several stereochemical pathways, both kinetically by the overall lowest barrier of 12.8 kcal mol^{-1} ($\Delta G^{\ddagger}$, Table 3), and also thermodynamically by the formation of the most stable η^3-*syn*,$\eta^1(C^1)$,Δ-*cis* isomer of **2**. The coupling of two *trans*-butadienes, which requires a slightly higher activation barrier ($\Delta G^{\ddagger}$ = 15.5 kcal mol^{-1}, Table 3), however, is a less likely process, since the highly strained, energetically disfavored η^3,$\eta^1(C^1)$,Δ-*trans* coupling species would immediately undergo the more facile reverse reductive decoupling **2** → **1b** process. Furthermore, formation of the η^3-*anti*,$\eta^1(C^1)$,Δ-*cis* isomer of **2** (*c*/*c*-butadiene coupling) is seen to be kinetically disabled by an activation barrier that is 4.9 kcal mol^{-1} ($\Delta\Delta G^{\ddagger}$, Table 3) higher, compared to the favorable *t*/*c*-butadiene (OF) coupling.

Comparison of the kinetics for the most feasible stereochemical pathways of the alternative **1a** → **4** and **1b** → **2** routes clearly shows that the octadienediyl−Ni^{II} complex is preferably generated via the ethylene-assisted coupling of two η^2-butadienes along **1b** → **2**. Thus, the thermodynamically favorable [$Ni^0(\eta^2$-butadiene$)_2$(ethylene)] form of **1b** also represents the catalytically active species for oxidative coupling. The [Ni^{II}-(η^3-*syn*,$\eta^1(C^1)$,Δ-*cis*-octadienediyl)(ethylene)] species **2** is almost exclusively formed[18] in a nearly thermoneutral process that requires a moderate activation barrier ($\Delta G^{\ddagger}$ = 12.8 kcal mol^{-1}), which indicates the oxidative coupling as a facile, reversible step. It should be noted that the ethylene- as well as the η^2-butadiene-assisted **1b** → **2** process has an almost identical intrinsic free-energy barrier (12.8 vs 12.6 kcal mol^{-1},[4c] relative to the [$Ni^0(\eta^2$-*trans*-butadiene$)_2$(ethylene)] and [$Ni^0(\eta^2$-*trans*-butadiene$)_3$] precursors, respectively), but the [$Ni^0(\eta^2$-butadiene$)_2$-(ethylene)] form is prevalent (vide supra).

B. Allylic Conversion Processes Occurring in the Octadienediyl−Ni^{II} Complex. The interconversion between the various configurations, viz., the η^3,η^1 species **2** and **3** and the bis(η^3) species **4**, as well as between the several stereoisomers of the octadienediyl−Ni^{II} complex may play a crucial role in the catalytic reaction course. Commencing from the initially generated η^3-*syn*,$\eta^1(C^1)$,Δ-*cis* species **2**, the subsequent generation of the decatrienyl−Ni^{II} complex can proceed with **2**, **3**, or **4** acting as the precursor. Furthermore, an isomer different from the *t*/*c*-butadiene OF coupling stereoisomer (cf. Table 3) can be involved along the most feasible pathway of this process. Therefore, provided that allylic conversion is kinetically impeded, several of the stereochemical pathways for formation of the decatrienyl−Ni^{II} complex would be disabled due to the negligible population of the corresponding precursor species.

The various octadienediyl−Ni^{II} configurations **2**−**4** are likely to readily undergo mutual conversion for identical stereoisomers.[19] Syn−anti isomerization as well as enantioface conversion of the terminal allylic groups are the most likely processes for interconverting different stereoisomeric forms. The transition-state structures encountered along the most feasible pathway for each of the two processes, respectively, are displayed in Figure 4 and the energetics of all investigated stereochemical pathways are collected in Table 4. The conversion of the allylic

(18) It should be noted that the same η^3,$\eta^1(C^1)$-octadienediyl−Ni^{II} stereoisomer has been unequivocally established as the initially formed coupling product for the PR_3/$P(OR)_3$-stabilized [$Ni^0(\eta^2$-butadiene$)_2$L] complex, which actively catalyzes the formation of C_8-cycloolefins (refs 3e, 6a, and 8).

(19) A facile rearrangement between different configurations has been observed by NMR for the PR_3/$P(OR)_3$-stabilized octadienediyl−Ni^{II} complex (ref 3e).

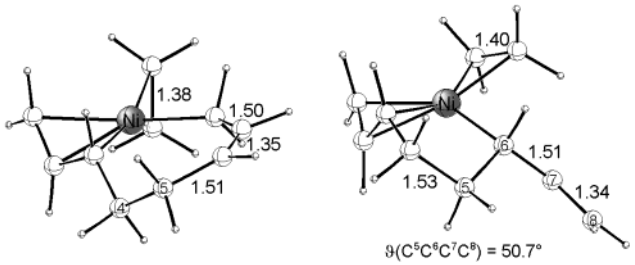

η^3-*syn*,η^1(C^1),Δ-*cis* TS$_{EFC}$[**2**] η^3-*syn*,η^1(C^3) TS$_{ISO}$[**3**]

Figure 4. Selected geometric parameters (angstroms) of the optimized η^3-*syn*,η^1(C^1) transition-state structure TS$_{EFC}$[**2**] for allylic enantioface conversion and of the optimized rotational η^3-*syn*,η^1(C^3) transition-state structure TS$_{ISO}$[**3**] for allylic isomerization to occur in the [Ni^{II}(octadienediyl)(ethylene)] complex.

Table 4. Activation Enthalpies and Free Energies for Allylic Isomerization via TS$_{ISO}$[**3**] with the [Ni^{II}(η^3,η^1(C^3)-octadienediyl)(ethylene)] Species **3** as Direct Precursor (top) and for Allylic Enantioface Conversion Occurring in the [Ni^{II}(η^3,η^1(C^1)-octadienediyl)(ethylene)] Species **2** (below)[a–d]

Allylic Isomerization			
isomer of **3**[e,f]		isomer of **3**[e,f]	TS$_{ISO}$[**3**]
η^3-*anti*,η^1(C^3)-*syn* [η^3-*anti*,η^1(C^1),Δ-*trans*]	⇌	η^3-*anti*,η^1(C^3)-*anti* [η^3-*anti*,η^1(C^1),Δ-*cis*]	
c/*t*-BD SF		*c*/*c*-BD OF	19.3/*19.2*
c/*t*-BD OF		*c*/*c*-BD SF	14.8/*14.7*
η^3-*syn*,η^1(C^3)-*anti* [η^3-*syn*,η^1(C^1),Δ-*cis*]	⇌	η^3-*syn*,η^1(C^3)-*syn* [η^3-*syn*,η^1(C^1),Δ-*trans*]	
t/*c*-BD SF		*t*/*t*-BD OF	**9.2**/***9.8***
t/*c*-BD OF		*t*/*t*-BD SF	11.9/*11.8*
Allylic Enantioface Conversion			
isomer of **2**[f]		isomer of **2**[f]	TS$_{EFC}$[**2**]
η^3-*syn*,η^1(C^1),Δ-*cis* *t*/*c*-BD SF	⇌	η^3-*syn*,η^1(C^1),Δ-*cis* *t*/*c*-BD OF	**10.1**/***10.7***
η^3-*anti*,η^1(C^1),Δ-*cis* *c*/*c*-BD SF	⇌	η^3-*anti*,η^1(C^1),Δ-*cis* *c*/*c*-BD OF	12.3/*12.6*

[a] This process is classified according to the butadiene coupling stereoisomers involved. The relationship between the butadiene coupling, and the stereoisomers of **2** and **3** is explicitly given. [b] Total barriers are relative to the prevalent isomer of **2**, namely, [Ni^{II}(η^3-*syn*,η^1(C^1),Δ-*cis*-octadienediyl)(ethylene)]. [c] Activation enthalpies and free energies ($\Delta H^{\ddagger}$/$\Delta G^{\ddagger}$) are given in kilocalories per mole; numbers in italic type are the Gibbs free energies. [d] The lowest barrier of the individual stereochemical pathway is shown in boldface type. [e] Corresponding stereoisomer of **2** is given in brackets. [f] See the text section Labeling of the Molecules for the BD coupling isomers listed.

enantioface was found to preferably proceed via the η^3,η^1(C^1)-octadienediyl−Ni^{II} transition state TS$_{EFC}$[**2**]. In accordance with evidence provided from both experimental[20,21] and theoretical[22] studies, allylic isomerization is most likely to occur via the η^3,η^1(C^3)-octadienediyl−Ni^{II} transition state TS$_{ISO}$[**3**], which constitutes the internal rotation of the vinyl group around the formal C^2−C^3 single bond. Neither TS$_{EFC}$[**2**] nor TS$_{ISO}$[**3**] is found to be stabilized by coordination of an additional ethylene or butadiene monomer at the enthalpic surface (ΔH). Therefore, it must be concluded that incoming monomers do not serve to accelerate the allylic conversion processes, and hence, additional monomers are not likely to participate in these processes.

The allylic enantioface conversion is indicated to be a facile process that is connected with similar free-energy barriers of 10.7 and 12.6 kcal mol^{-1} for *t*/*c*-butadiene and *c*/*c*-butadiene coupling stereoisomers, respectively (cf. Table 4). For allylic isomerization, however, the kinetics are found to be quite different for pathways that involve η^3-*syn*,η^1(C^3) isomers (i.e., conversion between *t*/*c*-butadiene and *t*/*t*-butadiene coupling products) and η^3-*anti*,η^1(C^3) isomers (i.e., conversion between *c*/*t*-butadiene and *c*/*c*-butadiene coupling products).[23] The first conversion has a moderate total barrier of 9.8−11.8 kcal mol^{-1} ($\Delta G^{\ddagger}_{tot}$, relative to the predominantly generated η^3-*syn*,η^1(C^1),Δ-*cis*,-octadienediyl−Ni^{II} species along **1b** → **2**, cf. Table 4), while the second stereochemical pathway requires a lowest barrier that is 4.9 kcal mol^{-1} higher ($\Delta\Delta G^{\ddagger}_{tot}$). This different behavior is almost entirely attributed to the lower thermodynamic stability of η^3-*anti*,η^1(C^3) relative to η^3-*syn*,η^1(C^3) isomers of the direct precursor **3**. Notably, both forms display comparable intrinsic reactivities, as indicated by similar intrinsic barriers of ∼7.5 kcal mol^{-1} ($\Delta G^{\ddagger}_{int}$, relative to the corresponding stereoisomer of **3**).

With the prevalent η^3,η^1(C^1),Δ-*cis*,-octadienediyl−Ni^{II} species **2** (where the two SF/OF stereoisomers are readily interconverted via facile allylic enantioface conversion, vide supra) as the starting point, a smooth conversion takes place into the *t*/*t*-butadiene coupling isomers ($\Delta G^{\ddagger}_{tot}$ = 9.8 kcal mol^{-1}). These species, however, are not likely to occur in significant stationary concentrations, as they undergo reductive decoupling **2** → **1b** readily (cf. section IA). The isomerization into *c*/*c*-butadiene coupling products is seen to be kinetically more difficult ($\Delta G^{\ddagger}_{tot}$ = 14.7 kcal mol^{-1}).[23]

C. Ethylene Insertion into the Allyl−Ni^{II} Bond of the Octadienediyl−Ni^{II} Complex. The decatrienyl−Ni^{II} complex can be generated following different paths for ethylene insertion into the Ni−C bond of the terminal allylic groups of the octadienediyl−Ni^{II} complex, with the η^3,η^1 configurations **2** and **3** and the bis(η^3) configuration **4** imaginable as precursors. Having probed various paths, the most favorable transition state located, in general, is characterized by a quasi-planar four-membered cis arrangement of the Ni−C bond, the ethylene, and the nickel atom. With the η^3,η^1(C^1) species **2** acting as precursor, ethylene can be inserted into either the η^3- or the η^1(C^1)-allyl−Ni^{II} bond. For both paths, a square-planar (SP) transition-state structure is encountered along the minimum energy pathway, in which ethylene resides in a square-planar conformation together with the η^3- and η^1(C^1)-allylic groups. A similar SP transition-state structure is also involved along the path for ethylene insertion into the η^3-allyl−Ni^{II} bond that starts from the η^3,η^1(C^3) species **3**. Furthermore, the alternative path that involves the bis(η^3) species **4** has been investigated. Commencing from several stereoisomers of the weakly bound square-pyramidal [Ni^{II}(bis(η^3)-octadienediyl)(ethylene)] ethylene adduct **4E**, in which ethylene adopts the axial position, inspection of the reaction path in a linear transit approach[24]

(20) Lukas, J.; van Leeuwen, P. W. N. M.; Volger, H. C.; Kouwenhoven, A. P. *J. Organomet. Chem.* **1973**, *47*, 153.
(21) (a) Faller, J. W.; Thomsen, M. E.; Mattina, M. J. *J. Am. Chem. Soc.* **1971**, *93*, 2642. (b) Vrieze, K. Fluxional Allyl Complexes. In *Dynamic Nuclear Magnetic Resonance Spectroscopy*; Jackman, L. M., Cotton, F. A., Eds.; Academic Press: New York, 1975.
(22) Tobisch, S.; Taube, R. *Organometallics* **1999**, *18*, 3045.
(23) The η^3-*syn*,η^1(C^3) (*t*/*c*-butadiene coupling) and η^3-*anti*,η^1(C^3) (*c*/*t*-butadiene coupling) isomers are connected by a facile η^3-*syn*,η^1-*anti* ⇌ η^3-*anti*,η^1-*syn* conversion. Linear transit calculations revealed no significant barrier for the process, thereby indicating that the intramolecular η^3/η^1 ⇌ η^1/η^3 shift proceeds readily.
(24) In the linear transit approach, the distance between the two carbon atoms of the newly formed C−C σ-bond was chosen as the reaction coordinate.

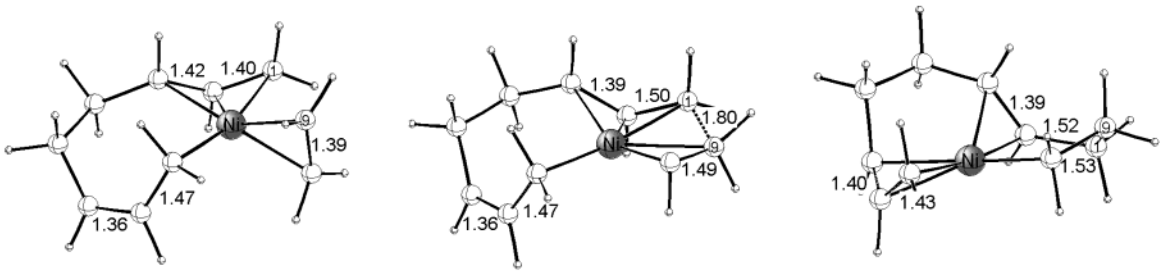

η^3-*syn*,η^1(C^1),Δ-*cis* **2** TS[**2**-**5**] η^3-*anti*,η^1,Δ-*trans* **5**

Figure 5. Selected geometric parameters (angstroms) of the optimized structures of key species for the feasible ethylene insertion into the *syn*-η^3-allyl−Ni^{II} bond along **2** → **5**.

Table 5. Activation Enthalpies and Free Energies and Reaction Enthalpies and Free Energies for Ethylene Insertion into the η^3-Allyl−Ni^{II} Bond and the η^1(C^1)-Allyl−Ni^{II} Bond of the Octadienediyl−Ni^{II} Intermediate **2** along **2** → **5**[a−d]

	ethene insertion path[e]		
BD coupling isomer[f]	**2**	TS[**2**–**5**]	**5**
ethene into *anti*-η^3-allyl	η^3-*anti*,η^1(C^1),Δ-*cis*		η^3-*anti*,η^1,Δ-*cis*
c/*c*-BD SF	1.0/*1.0*	19.3/*20.8*	10.9/*11.7*
c/*c*-BD OF	6.0/*6.0*	19.8/*21.3*	−5.3/*−3.7*
ethene into *syn*-η^3-allyl	η^3-*syn*,η^1(C^1),Δ-*cis*		η^3-*anti*,η^1,Δ-*trans*
t/*c*-BD SF	2.7/*2.7*	14.4/*15.8*	−8.7/*−7.0*
t/*c*-BD OF	0.0/*0.0*	**11.8**/***13.3***	**−12.6**/***−10.5***
	η^3-*syn*,η^1(C^1),Δ-*trans*		η^3-*syn*,η^1,Δ-*trans*
t/*t*-BD SF	12.5/*12.5*	21.7/*22.3*	−15.2/*−13.2*
t/*t*-BD OF	17.6/*17.6*	26.2/*26.8*	−11.7/*−9.9*
ethene into *anti*-η^1-allyl	η^3-*anti*,η^1(C^1),Δ-*cis*		η^3-*anti*,η^1,Δ-*cis*
c/*c*-BD SF	1.0/*1.0*	21.9/*23.0*	10.9/*11.7*
c/*c*-BD OF	6.0/*6.0*	29.6/*30.2*	−5.3/*−3.7*
ethene into *syn*-η^1-allyl	η^3-*syn*,η^1(C^1),Δ-*cis*		η^3-*syn*,η^1,Δ-*cis*
t/*c*-BD SF	2.7/*2.7*	22.4/*23.5*	−7.7/*−5.7*
t/*c*-BD OF	0.0/*0.0*	18.5/*19.7*	−5.9/*−4.1*
	η^3-*syn*,η^1(C^1),Δ-*trans*		η^3-*syn*,η^1,Δ-*trans*
t/*t*-BD SF	12.5/*12.5*	21.7/*22.3*	−15.2/*−13.2*
t/*t*-BD OF	17.6/*17.6*	26.2/*26.8*	−11.7/*−9.9*

[a] This process is classified according to the butadiene coupling stereoisomers involved. The relationship between the butadiene coupling and the stereoisomers of **2** and **5** is explicitly given. [b] Total barriers and reaction energies are relative to the prevalent isomer of **2**, namely, [Ni^{II}(η^3-*syn*,η^1(C^1),Δ-*cis*-octadienediyl)(ethylene)]. [c] Activation enthalpies and free energies ($\Delta H^{\ddagger}/\Delta G^{\ddagger}$) and reaction enthalpies and free energies ($\Delta H/\Delta G$) are given in kilocalories per mole; numbers in italic type are the Gibbs free energies. [d] The lowest barrier of the individual stereochemical pathway is shown in boldface type. [e] Ethene insertion path: ethene into *anti*-η^3-allyl, for example, denotes ethylene insertion into the *anti*-η^3-allyl−Ni^{II} bond in **2**. [f] See the text section Labeling of the Molecules.

revealed a smooth $\eta^3 \rightarrow \eta^1$ allylic rearrangement, in the vicinity of the transition state, of the group that is not directly involved in the process. The systems always approach the SP transition-state structure discussed above that corresponds to the ethylene insertion into the η^3-allyl−Ni^{II} bond of **2**.[25] Accordingly, bis-(η^3)-octadienediyl−Ni^{II} species do not participate along the energetically preferable ethylene insertion path.

Having excluded the path that starts from **4E** as a viable one, the two insertion paths with **2** and **3** as precursors are analyzed next. The energetic profiles are collected in Tables 5 and S1 (cf. Supporting Information), respectively. Inspection of the barriers associated with ethylene insertion into the η^3-allyl−Ni^{II} bond of **2** and **3** clearly predicts the path that starts from **2** as the favorable one of the two alternative paths, on kinetic grounds. For all the several stereochemical pathways, except for those with *t*/*t*-butadiene coupling octadienediyl−Ni^{II} species, lower free-energy barriers are calculated for formation of the decatrienyl−Ni^{II} complex, with **2** as the precursor. The preference of *t*/*t*-butadiene coupling species to follow the alternative insertion path is mainly attributed to the unfavorable steric strain associated with η^3-*syn*,η^1(C^1),Δ-*trans* isomers, which is less severe for the corresponding η^3-*syn*,η^1(C^3)-*syn* species. It should be noted, however, that these isomers (first) do not occur in appreciable concentration (vide supra) and (second) would also be kinetically precluded from feasible insertion pathways (vide infra). This leads to the conclusion that these species are not likely to play any role in the catalytic reaction course.

The careful inspection of the various insertion paths revealed that both the bis(η^3) species **4E** and the η^3,η^1(C^3) species **3** are precluded from the energetically most favorable path for ethylene insertion. Furthermore, for the operating path that commences from **2**, the η^3-allyl−Ni^{II} bond displays a higher aptitude for ethylene insertion when compared with the η^1(C^1)-allyl−Ni^{II} bond. This becomes evident from the fact that for identical stereoisomers the barrier for insertion into the η^3-allyl−Ni^{II} bond is predicted to always be lower than that for insertion into the η^1(C^1)-allyl−Ni^{II} bond (cf. Table 5).

The formation of the decatrienyl−Ni^{II} complex is seen to preferably proceed by ethylene insertion into the η^3-allyl−Ni^{II} bond of **2** via a SP transition state TS[**2**−**5**] that occurs at a distance of ∼1.8−1.9 Å for the emerging C−C σ-bond. This leads to the [Ni^{II}(η^3,η^1,Δ-decatrienyl)] species **5** as the kinetic insertion product, which represents the thermodynamically favorable one of the decatrienyl−Ni^{II} configurations **5**−**7**. Figure 5 shows the key species for the **2** → **5** step, the energetics of which are collected in Table 5 for all investigated stereoisomeric pathways.

Among the several stereoisomers of **2**, the predominantly generated η^3-*syn*,η^1(C^1),Δ-*cis* species (*t*/*c*-butadiene OF coupling along **1b** → **2**) is also seen to be the most reactive. Pathways with both OF and SF coupling stereoisomers, which are readily interconverted through smooth allylic enantioface conversion (cf. section IB), are indicated to be feasible. An activation energy of 13.3 and 15.8 kcal mol^{-1} ($\Delta G^{\ddagger}$) has to be overcome, affording the η^3-*anti*,η^1,Δ-*trans* isomer of **5**, in a process that is exergonic by −10.5 and −7.0 kcal mol^{-1}, respectively. The pathway with the *t*/*c*-butadiene OF coupling stereoisomer is preferable on both kinetic and thermodynamic grounds. On the other hand,

(25) The transition state that directly connects **4E** with the decatrienyl−Ni^{II} complex could not be located. It is, however, expected at significantly higher energies when compared to TS[**2**−**5**].

Table 6. Activation Enthalpies and Free Energies and Reaction Enthalpies and Free Energies for Reductive Elimination under CC−Bond Formation Affording CDD along **5** → **8**[a−d]

BD coupling isomer[e]	CDD-generating path		
	5	TS[**5**–**8**]	**8**
cis,*cis*-CDD	η^3-*anti*,η^1,Δ-*cis*		*cis*,*cis*-CDD
c/*c*-BD SF	23.5/*22.3*	53.8/*53.9*	32.9/*33.2*
c/*c*-BD OF	7.2/*6.8*	23.4/*24.3*	7.6/*7.9*
cis,*trans*-CDD	η^3-*anti*,η^1,Δ-*trans*		*cis*,*trans*-CDD
t/*c*-BD SF	3.9/*3.5*	**25.2**/***26.6***	17.7/*18.5*
t/*c*-BD OF	0.0/*0.0*	**26.6**/***27.9***	15.2/*16.1*
	η^3-*syn*,η^1,Δ-*cis*		*cis*,*trans*-CDD
t/*c*-BD SF	4.9/*4.8*	32.6/*33.7*	17.7/*18.5*
t/*c*-BD OF	6.7/*6.4*	31.8/*33.0*	15.2/*16.1*
trans,*trans*-CDD	η^3-*syn*,η^1,Δ-*trans*		*trans*,*trans*-CDD
t/*t*-BD SF	-2.6/-*2.7*	34.0/*34.8*	28.9/*29.6*
t/*t*-BD OF	0.8/*0.6*	37.2/*38.1*	31.0/*31.5*

BD coupling isomer[e]	*cis*,*trans*-CDD ethylene-assisted pathway[f]		
	5E	TS[**5E**-**8E**]	**8E**
t/*c*-BD SF	−2.5/*3.9*	**15.1**/***21.8***	−17.2/−*10.7*
t/*c*-BD OF	−0.7/*5.3*	**13.5**/***20.1***	−16.9/−*10.3*

[a] This process is classified according to the butadiene coupling stereoisomers involved. The relationship between the butadiene coupling, the stereoisomers of **5**, and the CDD stereoisomers formed is explicitly given. [b] Total barriers and reaction energies are relative to the prevalent isomer of **5**, namely, [Ni^{II}(η^3-*anti*,η^1,Δ-*trans*-decatrienyl)]. [c] Activation enthalpies and free energies ($\Delta H^{\ddagger}/\Delta G^{\ddagger}$) and reaction enthalpies and free energies ($\Delta H/\Delta G$) are given in kilocalories per mole; numbers in italic type are the Gibbs free energies. [d] The lowest barrier of the individual stereochemical pathway is shown in boldface type. [e] See the text section Labeling of the Molecules. [f] Total barriers and reaction energies for the ethylene-assisted path are given relative to {[Ni^{II}(η^3-*anti*,η^1,Δ-*trans*-decatrienyl)] isomer of **5** + C_2H_4}.

ethylene insertion into the *anti*-η^3-allyl−Ni^{II} bond of the η^3-*anti*,η^1(C^1),Δ-*cis* isomer of **2** (*c*/*c*-butadiene coupling species) is kinetically impeded due to distinctly higher activation barriers ($\Delta\Delta G^{\ddagger} > 7$ kcal mol^{-1}, cf. Table 5). As a consequence, the η^3-*anti*,η^1,Δ-*trans* isomer of the decatrienyl−Ni^{II} complex is generated nearly exclusively along **2** → **5**, while the formation of η^3,η^1,Δ-*cis*-decatrienyl−Ni^{II} species should be almost entirely precluded, mainly due to kinetic considerations. Thermodynamic grounds are seen to prevent occurrence of these species as well. The η^3-*anti*,η^1(C^1),Δ-*cis* precursor **2** is likely to be sparsely populated, since the compulsory allylic isomerization ($\Delta G^{\ddagger}_{tot}$ = 14.7 kcal mol^{-1}, cf. section IB) is indicated to be slower than the competitive ethylene insertion ($\Delta G^{\ddagger}$ = 13.3 kcal mol^{-1}).

The possible participation of additional monomers along **2** → **5** has been explicitly probed by the location of trigonal-bipyramidal [Ni^{II}(octadienediyl)(ethylene)$_2$] transition states for several of the stereochemical pathways. In neither case does additional ethylene serve to stabilize TS[**2**−**5**]; for instance, the transition states of the favorable stereochemical pathways are found to be 6.5 and 10.0 kcal mol^{-1} higher in enthalpy relative to {TS[**2**−**5**] + C_2H_4}. From this, it can be concluded that incoming monomers are not likely to assist the decatrienyl−Ni^{II} formation along **2** → **5**.

Identical stereoisomers (*t*/*c*-butadiene OF coupling) are found to participate along the most feasible pathways for oxidative coupling and ethylene insertion. Accordingly, allylic conversion in the octadienediyl−Ni^{II} complex is not necessary along the catalytic reaction course. Furthermore, the octadienediyl−Ni^{II} complex is indicated as a highly reactive intermediate occurring in low stationary concentrations, since the generating oxidative coupling and the consuming insertion processes are connected with similar moderate activation barriers. This leads to the conclusion that octadienediyl−Ni^{II} species are less likely to be isolable in the catalytic co-oligomerization reaction.

D. Allylic Isomerization Processes Occurring in the Decatrienyl−Ni^{II} Complex. Similar to the octadienediyl−Ni^{II} complex, the various decatrienyl−Ni^{II} configurations **5**−**7** are likely to be in a kinetically mobile equilibrium. The η^3-π-allyl form **5**, which is stabilized by the coordinated olefinic double bond, is prevalent, while **6** and **7** with a η^1-σ-allyl group are found to be thermodynamically disfavored. Having clarified that decatrienyl−Ni^{II} isomers with a trans double bond are almost exclusively formed along **2** → **5**, the interconversion between the prevalent *anti*-η^3-allyl form and its *syn*-η^3-allyl congener is investigated next. The activation barriers for this process are collected in Table S2 of the Supporting Information.

The allylic isomerization in the decatrienyl−Ni^{II} complex has been found to require assistance from additional monomers, which serve to compensate for the decrease of the coordination number of the nickel atom accompanied with the $\eta^3 \rightarrow \eta^1(C^3)$ allylic rearrangement. For the nonassisted process, an unrealistic energetic profile results with an artificially stabilized $\eta^1(C^3)$-allylic transition state that is caused by the lack of coordinative saturation. Anti−syn isomerization of the η^3-*anti*,η^1,Δ-*trans*-decatrienyl−Ni^{II} species via a $\eta^1(C^3)$-allyl rotational transition state requires a significant total barrier of 27.0 and 29.7 kcal mol^{-1} ($\Delta G^{\ddagger}_{tot}$ for the two stereoisomers, relative to the prevalent η^3-*anti*,η^1,Δ-*trans*,-decatrienyl−Ni^{II} isomer of **5**, cf. Table S2), for the process that is assisted by ethylene. This indicates the isomerization of the terminal allylic group of the decatrienyl−Ni^{II} complex to be a kinetically difficult process, which is likely to be impeded relative to the decatrienyl−Ni^{II} complex decomposition. The comparison of the energetics for these processes, which is investigated next, will clarify this aspect.

E. Formation of the C_{10}−Co-oligomers. At this stage of our systematic theoretical mechanistic study the competing routes for generation of linear and cyclic C_{10}-olefins are investigated. Exploration of several paths for each of the two routes, which commence from the various decatrienyl−Ni^{II} configuration **5**−**7**, clearly revealed that the η^3,η^1,Δ-*trans* form **5** acts as the precursor for the CDD and DT generating routes.

1. Formation of CDD. Formation of CDD proceeds along the most feasible path by establishing of a C−C σ-bond between the terminal unsubstituted carbons of the η^3-allylic (C^1) and the alkyl group (C^{10}) in **5** that affords the [Ni^0(CDD)] product complex **8**. The key species for generation of the 10-membered ring via reductive elimination along **5** → **8** are shown in Figure 6 and the energetics for all investigated stereochemical pathways are reported in Table 6. The transition state TS[**5**−**8**], which occurs at a distance of ∼1.9−2.1 Å of the newly formed bond, is characterized by a substantial η^3-allyl → vinyl transformation, such that the CDD product is already essentially formed. Thus TS[**5**−**8**] appears productlike and decays into the formal 14e$^-$ species **8** where CDD is coordinated to Ni^0 by its two double bonds.

The energetic profile (cf. Table 6) revealed the pathway with the η^3-*anti*,η^1,Δ-*cis*-decatrienyl−Ni^{II} isomer (*c*/*c*-butadiene OF coupling) involved as the most feasible among all of the stereochemical pathways. After surmounting a barrier of 24.3 kcal mol^{-1} ($\Delta G^{\ddagger}$) this would give rise to the *cis*,*cis*-CDD−Ni^0 product **8**. This pathway, however, is rendered inoperable, since

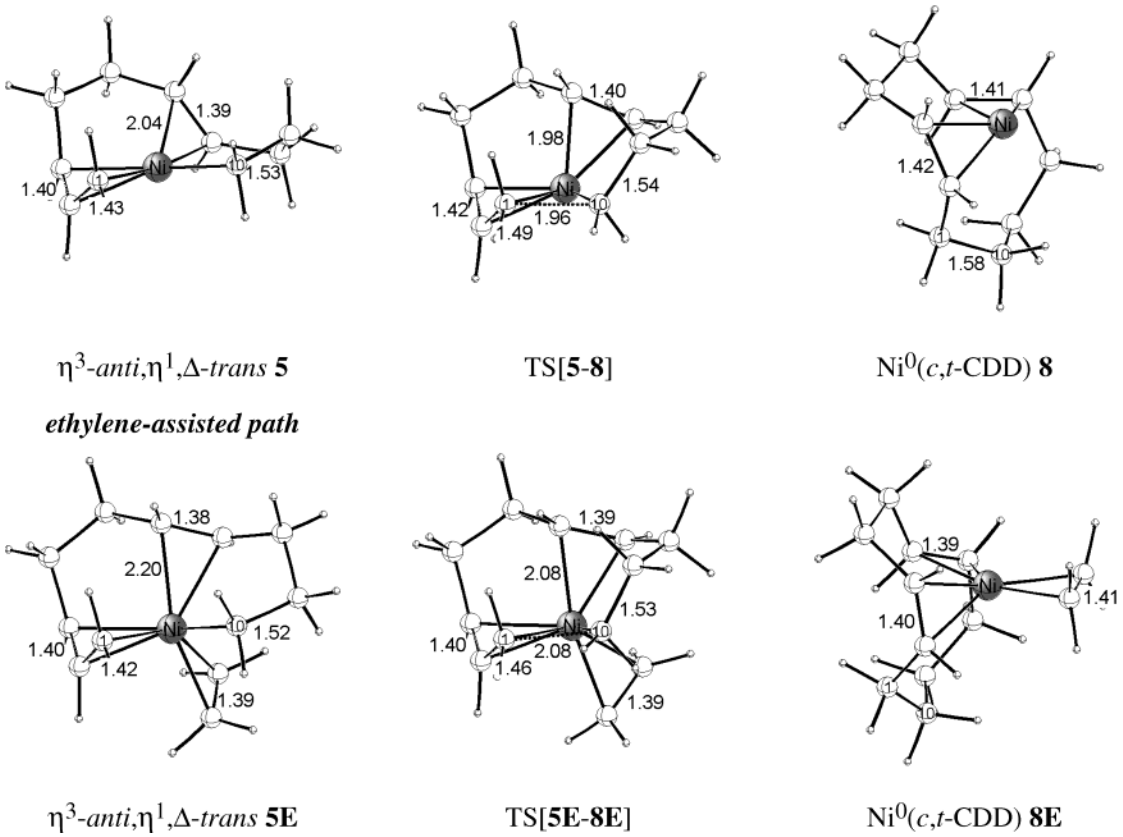

Figure 6. Top: Selected geometric parameters (angstroms) of the optimized structures of key species for reductive elimination affording *cis*,*trans*-CDD via the most feasible of the accessible stereochemical pathways along **5** → **8**. Bottom: Corresponding key species for the ethylene-assisted process.

the generation of the η^3,η^1,Δ-*cis* precursor **5** has been shown to be almost entirely precluded (cf. section IC). Among the accessible pathways with η^3,η^1,Δ-*trans*-decatrienyl−Ni^{II} isomers participating, the pathway with the prevalent η^3-*anti*,η^1,Δ-*trans* species is predicted to be favorable, on both kinetic and thermodynamic grounds. This gives rise to *cis*,*trans*-CDD as the preferable C_{10}-olefin along **5** → **8** that is generated in an endergonic process (ΔG = 18.5 and 16.1 kcal mol^{-1}) with a similar free energy of activation of 26.6 and 27.9 kcal mol^{-1} for the two SF and OF coupling stereoisomers, respectively. This barrier is seen to be in the same range as that predicted for allylic isomerization of the prevalent η^3-*anti*,η^1,Δ-*trans* species **5** (cf. section ID), thereby suggesting that the probability of the two processes occurring should be similar. Accordingly, the *trans*,*trans*-CDD generating pathway with the η^3-*syn*,η^1,Δ-*trans* precursor **5** becomes accessible. Formation of *trans*,*trans*-CDD, however, is clearly indicated to be kinetically unfeasible due to a barrier that is ∼8 kcal mol^{-1} higher ($\Delta\Delta G^{\ddagger}$). This leads to the following conclusions: (first) *cis*,*trans*-CDD is the preferably generated cyclic C_{10}-olefin along the **5** → **8** path that is (second) nearly exclusively formed among the different isomers, since all the other competing stereochemical pathways are almost entirely precluded due to kinetic and/or thermodynamic considerations. Furthermore, (third) isomerization of the terminal allylic group of the decatrienyl−Ni^{II} complex is not necessary along the reaction course.

As already indicated by the strong endergonicity of the reductive elimination, a process that formally goes along with a reduction of the coordination number on nickel, additional monomers are likely to participate via the **5** → **8** route. This has been probed explicitly for the process that is assisted by ethylene. Table 6 contains the energetics for the *cis*,*trans*-CDD generating pathway and Figure 6 shows the corresponding key species, on which we will exclusively focus here. The data for all the several stereochemical pathways are included in the Supporting Information (cf. Table S3). The incoming monomer has to compete for coordination with the coordinated olefinic double bond of the C_{10} chain. In the formally 16e^- square-planar η^3-*anti*,η^1,Δ-*trans* species **5**, additional ethylene shows a tendency to form stable square-pyramidal [Ni^{II}(η^3,η^1,Δ-*trans*-decatrienyl)(ethylene)] adducts **5E**, with ethylene adopting a position in the equatorial plane. The small enthalpic stabilization of **5E**, however, does not seem to be large enough to compensate for the decrease in entropy associated with ethylene complexation. In contrast, both TS[**5**−**8**] and **8** are found to be stabilized to a considerable extent by monomer coordination. The total free-energy barrier (relative to the separated prevalent η^3-*anti*,η^1,Δ-*trans* isomer of **5** and the olefin) is reduced to 20.1 and 21.3 kcal mol^{-1} for the favorable *cis*,*trans*-CDD generating pathway, which is now predicted to be exergonic, driven by a thermodynamic force of −10.3 and −8.9 kcal mol^{-1} (ΔG) for the process assisted by ethylene and η^2-*trans*-butadiene, respectively. Thus, ethylene is indicated to serve preferably to facilitate the *cis*,*trans*-CDD generating pathway, kinetically as well as thermodynamically, and is therefore likely to assist the **5** → **8** route. *Cis*,*trans*-CDD is liberated from **8E** through subsequent, consecutive substitution steps with butadiene in an overall exergonic process ($\Delta H/\Delta G$ = −9.2/−3.9 kcal mol^{-1}), which regenerates the active catalyst **1b**.

2. Formation of DT. Starting from the decatrienyl−Ni^{II} complex, the formation of *cis*- and *trans*-DT requires the transfer of a hydrogen atom from the alkyl end (β-H of the C^9 carbon)

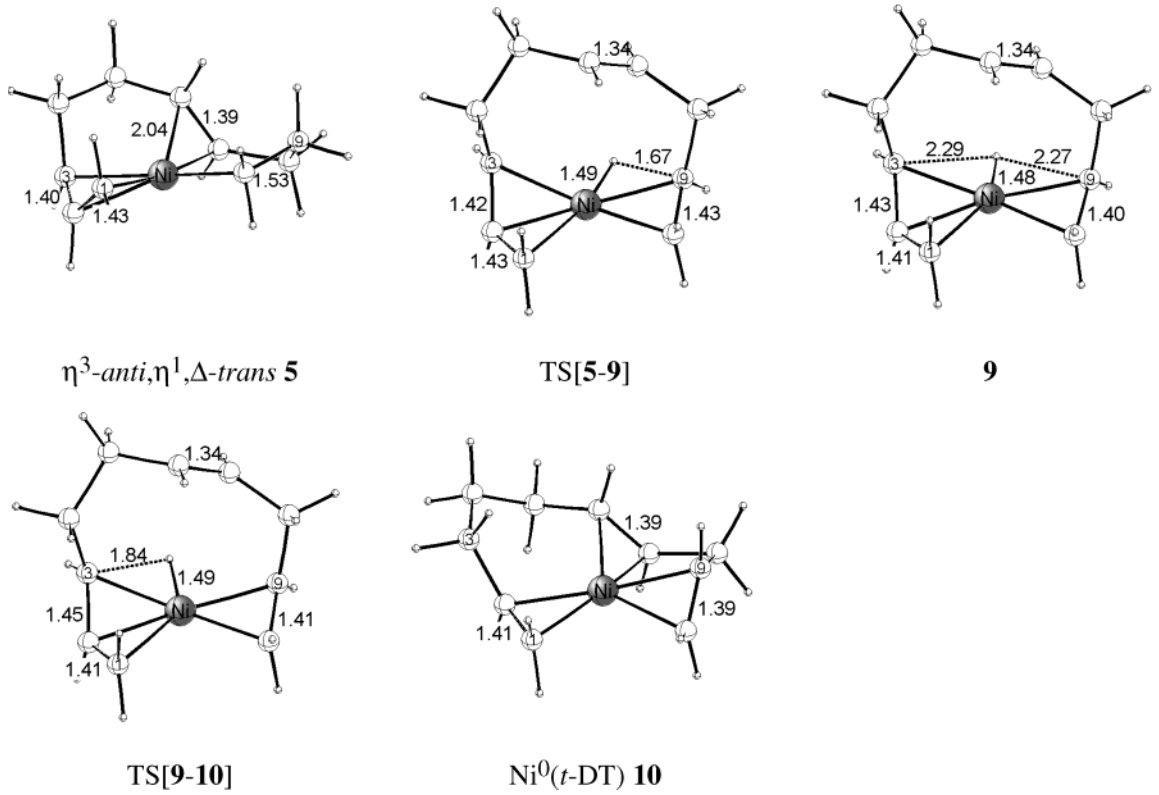

η^3-*anti*,η^1,Δ-*trans* **5** TS[**5**-**9**] **9**

TS[**9**-**10**] Ni^0(*t*-DT) **10**

Figure 7. Selected geometric parameters (angstroms) of the optimized structures of key species for the β-H abstraction **5** → **9** and reductive CH-elimination **9** → **10** steps affording *trans*-DT via the most feasible of the accessible stereochemical pathways along the overall **5** → **10** process.

to the allylic end (substituted C^3 carbon) of the C_{10} chain (cf. Figure 7). The probing of several reaction paths revealed that the favorable path, analogous to the findings in the previous section, starts from the η^3,η^1,Δ-*trans* species **5**, which represents the precursor for production of both cyclic and linear C_{10}-co-oligomers.[26] Furthermore, even an extensive search provided no indication of the existence of a viable concerted reaction path that excludes the intermediacy of the hydrido−Ni^{II} species **9**. Thus, the **5** → **9** → **10** sequence of steps represents the preferred path for DT generation that comprises the subsequent β-H abstraction **5** → **9** and reductive CH elimination **9** → **10** steps with the intervening hydrido−Ni^{II} species **9**. The corresponding localized key species are shown in Figure 7.

The hydrogen transfer preferably occurs coplanar to the η^3-allyl and the alkyl groups of the C_{10} chain, with the shifted hydrogen atom residing in square-planar conformation together with the two groups. The process is accompanied with the displacement of the inner-lying olefinic double bond, which is coordinated in **5**, from the immediate proximity of the nickel atom by the shifted hydrogen atom. The SP transition state TS[**5**−**9**] for the first β-H abstraction step is reached at the distance of ∼1.65−1.75 Å of the vanishing C^9−H^β bond and exhibits a hydrido−nickel bond (1.49 Å) that is almost completely established already, together with an emerging olefinic double bond on the alkyl terminus of the C_{10} chain. TS[**5**−**9**] decays into the stable SP hydrido−Ni^{II} intermediate **9**, which is confirmed to be a minimum. Both TS[**5**−**9**] and **9** display great structural similarity. Going further along the reaction path, TS[**9**−**10**] for reductive CH elimination is encountered at a distance of ∼1.8−1.9 Å of the new C−H bond, giving rise to the [Ni^0(DT)] complex **10**. After the hydrogen transfer along **5** → **10** succeeded with the creation of two new double bonds, the inner-lying double bond becomes recoordinated to the nickel atom; thus DT is coordinated by all its three double bonds to nickel in the formal $16e^-$ product **10**.

Table 7 reports the energetics for all accessible stereochemical pathways, namely, that with the η^3,η^1,Δ-*trans* isomers of **5** participating, on which the discussion is concentrated. The energetic profile for all stereochemical pathways is included in the Supporting Information (cf. Table S4). The **5** → **10** route for DT production, which occurs in two consecutive steps, exhibits a double valley profile. Very similar activation barriers are connected with the β-H abstraction and the reductive CH elimination, which amount to 20.0 and 18.7 kcal mol^{-1} ($\Delta G^{\ddagger}$), respectively, for the most feasible of the accessible stereochemical pathways with the prevalent η^3-*anti*,η^1,Δ-*trans* species **5** (*t*/*c*-butadiene OF coupling) participating. This leads to *trans*-DT in an overall process that is exergonic by −7.4 kcal mol^{-1}. The intervening hydrido−Ni^{II} species **9** is separated by a free-energy barrier of 2.7 and 1.4 kcal mol^{-1} from the educt and product sides. This indicates **9** as a highly reactive metastable intermediate that should be present only in negligible stationary concentrations.

From the moderate barriers for this preferred *trans*-DT generating pathway, it can be concluded that the alternative *trans*-DT pathway via η^3-*syn*,η^1,Δ-*trans* isomers of **5** is not reachable, due to the kinetically difficult (7.0 kcal mol^{-1} higher

(26) Whether the $\eta^1(C^3)$-σ-decatrienyl−Ni^{II} species **7** is involved along a practicable path for DT formation or not has been explicitly tested. The coordinatively unsaturated **7** is found to readily undergo $\eta^1(C^3) \rightarrow \eta^3$ allylic conversion, giving rise to the same key species that appear for the process commencing from **5**. Coordinative stabilization of **7** by ethylene complexation, however, leads to an alternative but energetically disfavored reaction path. Accordingly, **7** is precluded from the energetically most favorable path for DT formation.

Table 7. Activation Enthalpies and Free Energies and Reaction Enthalpies and Free Energies for β-H Abstraction and Subsequent Reductive CH Elimination Affording DT along **5** → **9** → **10**[a−d]

BD coupling isomer[e]	DT-generating path				
	5	TS[**5**–**9**]	**9**	TS[**9**–**10**]	**10**
trans-DT	η^3-*anti*,η^1,Δ-*trans*				*trans*-DT
t/*c*-BD SF	3.9/*3.5*	21.3/*20.7*	21.2/*20.0*	21.9/*21.2*	−6.0/−*6.7*
t/*c*-BD OF	0.0/*0.0*	**20.4**/***20.0***	18.2/*17.3*	**19.1**/***18.7***	**−6.6**/−***7.4***
trans-DT	η^3-*syn*,η^1,Δ-*trans*				*trans*-DT
t/*t*-BD SF	−2.6/−*2.7*	25.2/*24.8*	22.6/*21.5*	23.3/*22.8*	−8.9/−*9.4*
t/*t*-BD OF	0.8/*0.6*	28.9/*28.3*	26.9/*25.7*	27.6/*27.1*	−5.8/−*6.5*

BD coupling isomer[e]	*trans*-DT ethylene-assisted pathway[f]			
	5E	TS[**5E**–**9E**]	**9E**	TS[**9E**–**10E**]
t/*c*-BD SF	−2.5/*3.9*	24.2/*30.1*	21.7/*27.2*	22.7/*28.6*
t/*c*-BD OF	−0.7/*5.3*	**24.3**/***30.0***	21.3/*26.7*	**22.6**/***28.5***

[a] This process is classified according to the butadiene coupling stereoisomers involved. The relationship between the butadiene coupling, the stereoisomers of **5**, and the DT stereoisomers formed is explicitly given. [b] Total barriers and reaction energies are relative to the prevalent isomer of **5**, namely, [Ni^{II}(η^3-*anti*,η^1,Δ-*trans*-decatrienyl)]. [c] Activation enthalpies and free energies ($\Delta H^{\ddagger}/\Delta G^{\ddagger}$) and reaction enthalpies and free energies (ΔH/ΔG) are given in kilocalories per mole; numbers in italic type are the Gibbs free energies. [d] The lowest barrier of the individual accessible stereochemical pathway is shown in boldface type. [e] See the text section Labeling of the Molecules. [f] Total barriers and reaction energies for the ethylene-assisted path are given relative to {[Ni^{II}(η^3-*anti*,η^1,Δ-*trans*-decatrienyl)] isomer of **5** + C_2H_4}.

free-energy barrier, cf. section ID) but necessary anti−syn isomerization of the η^3,η^1,Δ-*trans* precursor **5**.

Among the two product isomers, *trans*-DT is the linear C_{10}-co-oligomer that is exclusively formed along **5** → **10** with the prevalent η^3-*anti*,η^1,Δ-*trans* (*t*/*c*-butadiene OF coupling) isomer of **5** involved, thus making allylic conversion in the decatrienyl−Ni^{II} precursor unnecessary. The competing *cis*-DT generating pathways with the η^3,η^1,Δ-*cis* isomers of **5** as precursors, are seen to be entirely precluded, although these species display a higher proclivity for undergoing H-transfer along **5** → **10** (cf. Table S4). Our critical analysis of crucial elementary steps clearly rationalizes the negligible thermodynamic population of η^3,η^1,Δ-*cis*-decatrienyl−Ni^{II} species (cf. section IC), as the decisive factor that prevents the generation of *cis*,*cis*-CDD and *cis*-DT, respectively.

Different from the **5** → **8** CDD-generating route, the production of DT is not likely to be facilitated by the participation of additional monomers along the **5** → **10** process. As evident from the energetics for the ethylene-assisted path (cf. Table 7 for the favorable *trans*-DT pathway and Table S5 for all stereochemical pathways), none of the key species is found to be coordinatively stabilized by monomer complexation, neither on the enthalpy nor on the free-energy surface.

Furthermore, the alternative hydrogen transfer path from the alkyl terminus (β-H of the C^9 carbon) to the unsubstituted C^1 allylic terminus of the C_{10} chain has been explicitly probed. Commencing from the prevalent η^3-*anti*,η^1,Δ-*trans* precursor **5**, this would give rise to deca-1,*trans*-4,*cis*-8,-triene (*trans*,*cis*-DT). In contrast to the *trans*-DT generating path, the first β-H abstraction proceeds through a SP transition-state structure with the shifting H-atom in axial position. This path is clearly seen to be almost entirely precluded kinetically, as it requires a free-energy barrier that is 19.5 kcal mol^{-1} higher ($\Delta\Delta G^{\ddagger}$) than that for the favorable *trans*-DT generating path.

II. Theoretically Verified and Refined Catalytic Cycle. A. Free-Energy Profile. On the basis of the careful theoretical exploration of important elementary processes of the tentative catalytic cycle, reported in previous sections, we now present the free-energy profile (cf. Scheme 2) of the complete reaction course for the co-oligomerization of 1,3-butadiene and ethylene mediated by zerovalent bare nickel complexes. It consists of the most feasible path for individual elementary steps.

The formal 16e$^-$ trigonal planar [Ni^0(η^2-butadiene)$_2$(ethylene)] species **1b** is the prevalent form of the active catalyst, with the bis(η^2-*trans*) isomers being most stable, which also represents the catalytically active form for oxidative coupling. Oxidative coupling is preferably to proceed via establishment of a C−C σ-bond between the terminal noncoordinated carbons of the two η^2-butadienes, giving rise to the [Ni^{II}(η^3,η^1(C^1),Δ,-octadienediyl)(ethylene)] species **2** as the initial product along the ethylene-assisted **1b** → **2** path. The most feasible pathway occurs via *t*/*c*-butadiene coupling, possessing a moderate kinetic barrier that affords the thermodynamically favored η^3-*syn*,η^1(C^1),Δ-*cis* isomer of **2** in a thermoneutral process. This indicates the oxidative coupling as a facile, reversible process. The alternative pathways for coupling of two *cis*-butadienes (kinetically impeded) and of two *trans*-butadienes (the more facile reverse **2** → **1b** process) are pointed out to be less likely. From this, together with the kinetically difficult conversion between η^3-*syn*,η^1(C^1),Δ-*cis* and η^3-*anti*,η^1(C^1),Δ-*cis* isomers, it can be concluded that the η^3-*syn*,η^1(C^1),Δ-*cis* species is the almost exclusively occurring isomer of **2**, while the η^3-*syn*,η^1(C^1),Δ-*trans* and η^3-*anti*,η^1(C^1),Δ-*cis* species are expected to be in negligible concentrations.

The dominant decatrienyl−Ni^{II} production path proceeds through the insertion of ethylene into the η^3-allyl−Ni^{II} bond of **2** that encounters a square-planar transition state. This gives rise to η^3,η^1,Δ-decatrienyl−Ni^{II} species **5** as the kinetic insertion product, which represents the thermodynamically favorable form of the decatrienyl−Ni^{II} complex. A moderate activation barrier, which is very similar to that for oxidative coupling, is connected with the most feasible insertion pathway, thereby indicating the octadienediyl−Ni^{II} complex as a highly reactive intermediate. Identical stereoisomers participate along the most feasible pathways for these two steps, thus making possible intervening allylic conversion processes in the octadienediyl−Ni^{II} complex unnecessary. Ethylene insertion into the *syn*-η^3-allyl−Ni^{II} bond of the prevalent η^3,η^1(C^1),Δ-*cis* isomer of **2** leads to the η^3-*anti*,η^1,Δ-*trans* isomer of **5** in an exergonic, irreversible process.

The formation of allyl,η^1,Δ-*cis*-decatrienyl−Ni^{II} species, however, is shown to be almost entirely disabled, because of (first) the negligible thermodynamic population of the corresponding η^3-*anti*,η^1,Δ-*cis* precursor species **2** (vide supra) and (second) a kinetically impeded ethylene insertion along this stereochemical pathway. Consequently, the *cis*,*cis*-CDD and *cis*-DT generating paths are entirely precluded. This explains why these product isomers are not observed in the catalytic co-oligomerization process.

The η^3-allyl,η^1,Δ-*trans*-decatrienyl−Ni^{II} form of **5** represents the precursor for the competing routes for generation of both linear and cyclic C_{10}-olefins. CDD is formed via reductive elimination, where the C_{10} cycle has been shown to be preferably generated through the establishment of a C−C σ-bond between the terminal carbons of the η^3-allyl and alkyl groups along

Scheme 2. Condensed Gibbs Free-Energy Profile of the Complete Catalytic Cycle of the [Ni^0]-Catalyzed Co-oligomerization of 1,3-Butadiene and Ethylene Affording Linear and Cyclic C_{10}-Olefins[a]

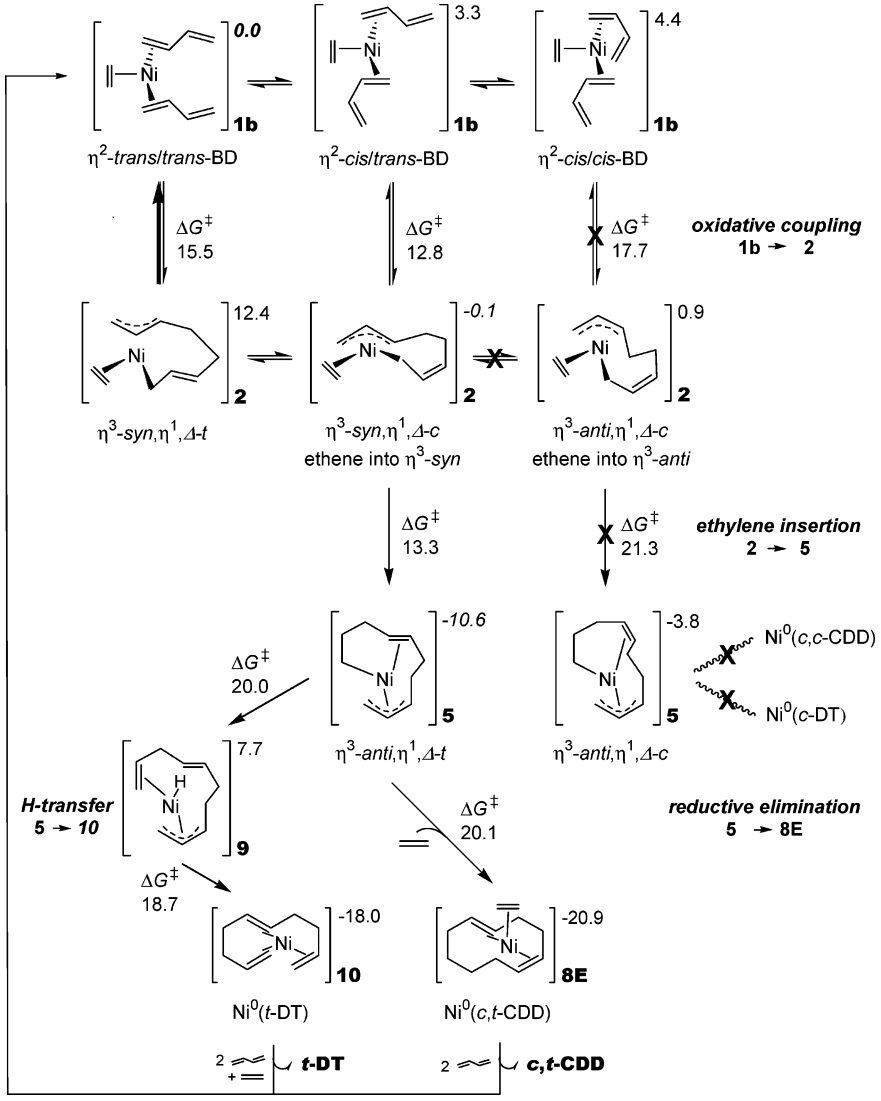

[a] The cycle is focused on viable routes for individual elementary steps. The favorable [$Ni^0(\eta^2$-*trans*-butadiene)$_2$(ethylene)] isomer of the active catalyst **1b** was chosen as reference. Activation barriers for individual steps are given in kilocalories per mole relative to the favorable stereoisomer of the respective precursor (given in italic type)

5 → **8**. On the other hand, the DT generating route **5** → **10** involves a stepwise transition-metal-assisted $C^9 \rightarrow C^3$ H-transfer, with a metastable hydrido−Ni^{II} species **9** participating. The formation of linear and cyclic C_{10}-olefins occurs in a highly stereoselective fashion. Among the several isomers, *cis*,*trans*-CDD and *trans*-DT are generated almost exclusively along **5** → **8** and **5** → **10**, respectively, with the prevalent η^3-*anti*,η^1,Δ-*trans* isomer of **5** as the precursor.

The DT generating route is shown to be unassisted by incoming monomers. The transition state TS[**5**−**8**] and also **8**, however, are substantially stabilized by ethylene complexation, leading to a significant acceleration of the CDD generating route. With the thermodynamically favorable species **5** as the precursor, the *cis*,*trans*-CDD and *trans*-DT generating pathways are connected with the largest overall kinetic barrier among all the critical elementary steps, affording the [$Ni^0(\eta^4$-CDD)(ethylene)] and [$Ni^0(\eta^6$-DT)] products **8E** and **10**, respectively, in an exergonic irreversible process. Accordingly, the **5** → **8E** and **5** → **10** decomposition of the decatrienyl−Ni^{II} complex to afford cyclic and linear C_{10}-olefins, which display similar kinetics, is predicted to be rate-controlling. The free-energy barrier of 20.1 and 20.0 kcal mol^{-1}, respectively, for these steps corresponds very well with experimental estimates[27] and shows that production of C_{10}-co-oligomers requires moderate reaction conditions.[5]

The C_{10}-co-oligomer products are liberated in subsequent, consecutive substitution steps with new ethylene and butadiene monomers, which are exothermic by −9.2 and −9.3 kcal mol^{-1} (ΔH) for expulsion of *cis*,*trans*-CDD and *trans*-DT from **8E** and **10**, respectively, by the required monomers to recreate the active form of **1b**. Overall, the co-oligomerization process is driven by a strong thermodynamic force with an exothermicity of −41.4 and −31.2 kcal mol^{-1} (ΔH for the noncatalyzed

(27) The overall free energy of activation for the [Ni^0]-catalyzed co-oligomerization of 1,3-butadiene and ethylene has been estimated from available experimental data (ref 5a) by the following crude approximation: with a TOF of 12.7 g of C_{10}-olefin (g of Ni)$^{-1}$ h^{-1} at 313 K (with *cis*,*trans*-CDD as the predominant product) and of 370 g of C_{10}-olefin (g of Ni)$^{-1}$ h^{-1} at 353 K (with *trans*-DT as the predominant product), one obtains effective rate constants $k \sim 1.52 \times 10^{-3}/4.43 \times 10^{-2}$ s^{-1} and $\Delta G^{\ddagger} \sim 22.4/22.9$ kcal mol^{-1}, respectively, by applying the Eyring equation with $k = (2.08 \times 10^{10})T \exp(-\Delta G^{\ddagger}/RT)$.

process) for the linkage of two *trans*-butadiene and one ethylene monomers to afford *cis*,*trans*-CDD and *trans*-DT, respectively.

B. Regulation of the Distribution between Linear and Cyclic C_{10}-Olefins. As analyzed in the previous section, the decomposition of **5**, occurring along competing routes for production of linear and cyclic C_{10}-olefins, is rate-controlling in the overall co-oligomerization reaction, which furthermore involves identical stereoisomers. Accordingly, the product selectivity is entirely regulated kinetically by the difference of the highest overall barrier ($\Delta\Delta G^{\ddagger}$) for the competing *cis*,*trans*-CDD and *trans*-DT generating pathways.

As is evident from the free-energy profile (cf. Scheme 2), the two pathways are predicted to be very similar in both the kinetic and the thermodynamic aspects. On the basis of the almost identical predicted free-energy barriers ($\Delta\Delta G^{\ddagger} = 0.1$ kcal mol^{-1}), the two pathways should be crossed in comparable probabilities, giving rise to an approximate 1:1 ratio of linear and cyclic C_{10}-co-oligomers. This seems contradictory to experiment, where *cis*,*trans*-CDD is observed as the predominant product at low temperatures.[5b] The production of CDD, however, is likely to be assisted by incoming ethylene, while the DT generating route is not. The prediction of accurate free energies for transition-metal-assisted processes in condensed phase remains a challenge for computational chemistry, in particular when species of different stoichiometry are involved. Due to the uncertainty in the estimated entropic costs for monomer association and dissociation processes (cf. Computational Model and Method section), caused by the theoretical methodology employed in the present study, the computed $\Delta\Delta G^{\ddagger}$ value for the subtle energetic balance[28] between the two competing pathways does not exactly reproduce the experimentally observed product ratio between linear and cyclic C_{10}-co-oligomers.

The presented theoretical−mechanistic investigation, however, allows a detailed understanding and a consistent rationalization of the experimental results. As already outlined in the Introduction, temperature and ethylene pressure are the dominant factors that regulate the selectivity of the co-oligomerization. The computed $\Delta\Delta G^{\ddagger}$ value increases to 1.4 kcal mol^{-1} (353 K) at higher temperatures, with the **5** → **10** route having the lower barrier. Accordingly, production of *trans*-DT is indicated to become kinetically favorable at elevated temperatures, which is consistent with experimental findings.[5] Our analysis revealed that both low temperatures (entropic effect) and high ethylene pressure (assistance of the **5** → **8E** route) serve to favor the *cis*,*trans*-CDD generation. Accordingly, for the co-oligomerization occurring at room temperature the CDD selectivity can be enhanced by increasing the ethylene pressure. Furthermore, *cis*,*trans*-CDD should be the major C_{10}-olefin at elevated temperatures as well, provided that the ethylene pressure is high enough to compensate for the entropic disfavor. On the other hand, *trans*-DT should be predominantly formed at low ethylene pressure (together with larger portions of *all-t*-CDT), even at low temperatures.

(28) It should be noted that the experimentally observed 88:12 C_{10}-product ratio (ref 5b) corresponds to a $\Delta\Delta G^{\ddagger}$ value of only 1.16 kcal mol^{-1} (293 K).

Concluding Remarks

We have presented a detailed theoretical mechanistic investigation of the complete catalytic reaction course for the co-oligomerization of 1,3-butadiene and ethylene to afford linear and cyclic C_{10}-olefin products with a zerovalent bare nickel catalyst. Crucial elementary processes have been critically scrutinized for a tentative catalytic cycle (cf. Scheme 1) by means of a gradient-corrected DFT method. The original mechanistic proposal was confirmed in essential details but enhanced and supplemented by novel insights into how the co-oligomerization reaction operates (cf. sections IIA and IIB). The following have been achieved: (1) the most feasible among the various conceivable paths for each of the important elementary steps has been predicted, with special emphasis directed to the several stereochemical pathways; (2) the role played by the various configurations of the octadienediyl−Ni^{II} and decatrienyl−Ni^{II} complexes within the catalytic reaction course has been clarified; (3) the origin for the highly stereoselective formation of *cis*,*trans*-CDD and *trans*-DT, respectively, as the exclusively generated isomers of cyclic and linear C_{10}-olefin products has been rationalized; and (4) an enhanced insight into the regulation of the selectivity of the production of linear and cyclic C_{10}-olefins has been provided.

This leads us to propose a theoretically verified, refined catalytic cycle for production of linear and cyclic C_{10}-olefin products (cf. Scheme 2). The present theoretical mechanistic investigation contributes (first) to a more detailed understanding of mechanistic aspects of the [Ni^0]-mediated co-oligomerization of 1,3-dienes and olefins and (second) to a deeper insight into the catalytic structure−reactivity relationships in the transition-metal-assisted oligomerization and co-oligomerization reactions of 1,3-dienes.

Acknowledgment. I wish to thank Professor Tom Ziegler (University of Calgary, Canada) for his generous support. Excellent service by the computer centers URZ Halle and URZ Magdeburg is gratefully acknowledged.

Supporting Information Available: Full descriptions of the geometry of all reported key species (Cartesian coordinates in angstroms) and the complete collection of the results for all investigated stereochemical pathways for several of the elementary steps (PDF). This material is available free of charge via the Internet at http://pubs.acs.org.

JA0388865